

**Louisiana Water Resources Research Institute
Annual Technical Report
FY 2013**

Introduction

This report presents a description of the activities of the Louisiana Water Resources Research Institute for the period of March 1, 2013 to February 28, 2014 under the direction of Dr. John Pardue. The Louisiana Water Resources Research Institute (LWRRRI) is unique among academic research institutions in the state because it is federally mandated to perform a statewide function of promoting research, education and services in water resources. The federal mandate recognizes the ubiquitous involvement of water in environmental and societal issues, and the need for a focal point for coordination.

As a member of the National Institutes of Water Resources, LWRRRI is one of a network of 54 institutes nationwide initially authorized by Congress in 1964 and has been re-authorized through the Water Resources Research Act of 1984, as amended in 1996 by P.L. 104-147. Under the Act, the institutes are to:

"1) plan, conduct, or otherwise arrange for competent research that fosters, (A) the entry of new research scientists into water resources fields, (B) the training and education of future water scientists, engineers, and technicians, (C) the preliminary exploration of new ideas that address water problems or expand understanding of water and water-related phenomena, and (D) the dissemination of research results to water managers and the public.

2) cooperate closely with other colleges and universities in the State that have demonstrated capabilities for research, information dissemination and graduate training in order to develop a statewide program designed to resolve State and regional water and related land problems. Each institute shall also cooperate closely with other institutes and organizations in the region to increase the effectiveness of the institutes and for the purpose of promoting regional coordination."

The National Water Resources Institutes program establishes a broad mandate to pursue a comprehensive approach to water resource issues that are related to state and regional needs. Louisiana is the water state; no other state has so much of its cultural and economic life involved with water resource issues. The oil and gas industry, the chemical industry, port activities, tourism and fisheries are all dependent upon the existence of a deltaic landscape containing major rivers, extensive wetlands, numerous large shallow water bays, and large thick sequences of river sediments all adjacent to the Gulf of Mexico.

Louisiana has an abundance of water resources, and while reaping their benefits, also faces complex and crucial water problems. Louisiana's present water resources must be effectively managed, and the quality of these resources must be responsibly protected. A fundamental necessity is to assure continued availability and usability of the state's water supply for future generations. Specifically, Louisiana faces five major issues that threaten the quality of the state's water supply, which are also subsets of the southeastern/island region priorities:

Nonpoint sources of pollution are estimated to account for approximately one-half of Louisiana's pollution. Because of the potential impact of this pollution and the need to mitigate its effects while maintaining the state's extensive agricultural base and coastal zones, continued research is needed in the area of nonpoint issues. Louisiana's regulatory agencies are addressing non-point source problems through the development of waste load allocation models or total maximum daily load (TMDL) calculations. There are serious technical issues that still require resolution to insure that progress is made in solving the non-point source problem.

Louisiana's vast wetlands make up approximately 40% of the nation's wetlands. These areas are composed of very sensitive and often delicately balanced ecosystems which make them particularly vulnerable to contamination or destruction resulting both from human activities and from natural occurrences. Understanding these threats and finding management alternatives for the state's unique wetland resources are

priority issues needing attention.

Water resources planning and management are ever-present dilemmas for Louisiana. Severe flooding of urban and residential areas periodically causes economic loss and human suffering, yet solutions to flooding problems can be problems in themselves. Water supply issues have also recently a focus of concern. Despite the abundance of resources, several aquifers have been in perennial overdraft, including the Chicot aquifer. Louisiana passed its first legislation that restricts groundwater use in the past year. Water resources and environmental issues are intricately interconnected; therefore, changes in one aspect produce a corresponding responsive change in another. Further study is needed to understand these relationships.

Water quality protection, particularly of ground water resources, is an area of concern in Louisiana. Researchers are beginning to see contamination in drinking water supplies that was not present in the past. Delineating aquifer recharge areas, understanding the impacts of industrial activities on water resources, evaluating nonpoint sources of pollution, and exploring protection alternatives are issues at the forefront.

Wastewater management has been a long-standing issue in Louisiana. The problem of wastewater management focuses primarily on rural and agricultural wastewater and the high costs for conventional types of wastewater treatment as found in the petrochemical industry.

The Institute is administratively housed in the College of Engineering and maintains working relationships with several research and teaching units at Louisiana State University. Recent cooperative research projects have been conducted with Tulane University, Texas Tech University the EPA's Hazardous Substance Research Center- South & Southwest.

During this reporting period, LWRRRI continued its work on the Deepwater Horizon oil spill. The LWRRRI director advised state and national agencies, conducted ongoing research on the fate of oil in the systems and organized and presented research results at local, regional and national meetings. Details of this activity are presented below in the "Notable Achievements" section of the report.

Research Program Introduction

The primary goal of the Institute is to help prepare water professionals and policy makers in the State of Louisiana to meet present and future needs for reliable information concerning national, regional, and state water resources issues. The specific objectives of the Institute are to fund the development of critical water resources technology, to foster the training of students to be water resources scientists and engineers capable of solving present and future water resources problems, to disseminate research results and findings to the general public, and to provide technical assistance to governmental and industrial personnel and the citizens of Louisiana.

The priority research areas for the Institute in FY 2013 focused on selected research themes developed in conjunction with the advisory board. These themes corresponded to the major water resource areas affecting Louisiana described in the Introduction above. Projects selected were from a range of faculty with different academic backgrounds including geological scientists, environmental engineers and water resource engineers and scientists. Supporting research in these priority areas has increased the visibility of the Institute within the State.

The individual research projects designated as Projects 2013LAXXXX, are listed below.

Project 2010LA76G, Tsai & Hanor - Hierarchical Multimodel Saltwater Intrusion Remediation and Sampling Designs: A BMA Tree Approach

Project 2013LA93B - Malone and Adrian, Sustainable Iron Removal from Groundwaters Supporting Aquaculture

Project 2013LA92B - Deng, Development of Total Maximum Daily Load for Dissolved Oxygen in Nutrient-Enriched Lowland Rivers Project 2013LA91B - Tsai, Hydrostratigraphy Modeling of the Southern Hills Aquifer System

These projects include one project that focus on engineering (Project 2013LA93B), two projects that focus on groundwater flow and transport (Projects 2010LA76G and 2013LA91B), and one project that focuses on water quality (Project 2013LA92B).

Hierarchical Multimodel Saltwater Intrusion Remediation and Sampling Designs: A BMA Tree Approach

Basic Information

Title:	Hierarchical Multimodel Saltwater Intrusion Remediation and Sampling Designs: A BMA Tree Approach
Project Number:	2010LA76G
Start Date:	9/1/2010
End Date:	8/31/2013
Funding Source:	104G
Congressional District:	Louisiana
Research Category:	Ground-water Flow and Transport
Focus Category:	Groundwater, Management and Planning, Methods
Descriptors:	
Principal Investigators:	Frank Tsai, Jeff Hanor

Publications

1. Tsai, F.T.-C. (2011). Scavenger Wells Stop Saltwater Intrusion in Baton Rouge, Louisiana, IGWMC MODFLOW and More 2011 Conference: Integrated Hydrologic Modeling, Golden, Colorado, June 5-8, 2011.
2. Tsai, F. T.-C., and Ahmed S. Elshall (2011). A Hierarchical Bayesian Model Averaging Approach to Cope With Sources of Uncertainty in Conceptual Ground Water Models, World Water & Environmental Resources Congress, Palm Springs, California, May 22-26, 2011.
3. Tsai, F. T.-C. (2011). Stop Saltwater Intrusion Toward Water Wells Using Scavenger Wells, World Water & Environmental Resources Congress, Palm Springs, California, May 22-26, 2011.
4. Callie E. Anderson and Jeffrey S. Hanor (2011) Origin of waters causing salinization of the Baton Rouge aquifer system, Louisiana. South-Central Section Geological Society of America 45th Annual Meeting, March 27-29, 2011.
5. Frank T.-C. Tsai (2011). Saltwater Intrusion Simulation in the “1,500-Foot” Sand of the Baton Rouge Area: Pre-Anthropogenic Pumping, Current Situation, Future, Fifth Annual Louisiana Groundwater, Coastal Geology and Subsidence-Land Loss Symposia, Baton Rouge, Louisiana, January 11-12, 2011.
6. Callie E. Anderson and Jeffrey S. Hanor (2011) The St. Gabriel salt dome as a potential source of the salty waters contaminating the Baton Rouge aquifer system. Fifth Annual Louisiana Groundwater, Coastal Geology and Subsidence-Land Loss Symposia, Baton Rouge, Louisiana, January 11-12, 2011.
7. Ahmed Elshall and Frank T.-C. Tsai (2011). Geophysical and geostatistical approaches to subsurface characterization of the Baton Rouge area, Fifth Annual Louisiana Groundwater, Coastal Geology and Subsidence-Land Loss Symposia, Baton Rouge, Louisiana, January 11-12, 2011.
8. Nima Chitsazan and Frank T.-C. Tsai (2011). Bed boundary delineation of “1,500-foot”, “1,700-foot”, and “2,000-foot sands of the Baton Rouge area, Fifth Annual Louisiana Groundwater, Coastal Geology and Subsidence-Land Loss Symposia, Baton Rouge, Louisiana, January 11-12, 2011.
9. Tsai, F. T.-C. (2010). “1,500-Foot” Sand Saltwater Intrusion Simulation and Management Using Scavenger Wells, Baton Rouge Geological Society, Baton Rouge, Louisiana, December 10, 2010. (invited)

Hierarchical Multimodel Saltwater Intrusion Remediation and Sampling Designs: A BMA Tree Approach

10. Tsai, F.T.-C. (2010), Scavenger Wells Stop Saltwater Intrusion in Baton Rouge, 2010 Louisianan Water Quality Technology Conference, Alexandria and Baton Rouge, Louisiana, December 14-15, 2010. (invited)
11. Tsai, F.T.-C. (2010) Scavenger Well Operation to Stop Saltwater Intrusion Toward BRWC Lula Wells in the Baton Rouge Area, Louisiana Capital Area Ground Water Conservation Commission, September 14, 2010. (invited)
12. • Frank Tsai, 2012, Feasibility Study of Scavenging Approach to Stop Saltwater Toward Water Wells, Louisiana State University, Baton Rouge, Louisiana, 10 pages. (USGS 104B)
13. Tsai, F. T.-C., and A.S. Elshall. (2011). A Hierarchical Bayesian Model Averaging Approach to Cope With Sources of Uncertainty in Conceptual Ground Water Models, World Water & Environmental Resources Congress, Palm Springs, CA, May 22-26, 2011.
14. Tsai, F. T.-C. (2011). Development of Scavenger Well Operation Model To Stop Saltwater Intrusion Toward Water Wells In The “1,500-Foot” Sand of The Baton Rouge Area, Louisiana, World Water & Environmental Resources Congress, Palm Springs, CA, May 22-26, 2011.
15. Tsai, F. T.-C. (2011). Scavenger Wells Stop Saltwater Intrusion in Baton Rouge, Louisiana, MODFLOW and More 2011, Golden, CO, June 5-8, 2011
16. • Frank Tsai, 2012, Feasibility Study of Scavenging Approach to Stop Saltwater Toward Water Wells, Louisiana State University, Baton Rouge, Louisiana, 10 pages. (USGS 104B)
17. Tsai, F. T.-C., and A.S. Elshall. (2011). A Hierarchical Bayesian Model Averaging Approach to Cope With Sources of Uncertainty in Conceptual Ground Water Models, World Water & Environmental Resources Congress, Palm Springs, CA, May 22-26, 2011.
18. Tsai, F. T.-C. (2011). Development of Scavenger Well Operation Model To Stop Saltwater Intrusion Toward Water Wells In The “1,500-Foot” Sand of The Baton Rouge Area, Louisiana, World Water & Environmental Resources Congress, Palm Springs, CA, May 22-26, 2011.
19. Tsai, F. T.-C. (2011). Scavenger Wells Stop Saltwater Intrusion in Baton Rouge, Louisiana, MODFLOW and More 2011, Golden, CO, June 5-8, 2011
20. Elshall, A. S., F. T.-C. Tsai, J. S. Hanor, Indicator geostatistics for reconstructing Baton Rouge aquifer-fault hydrostratigraphy (Louisiana, USA), Hydrogeology Journal, 2013. (accepted)
21. Tsai, F. T.-C. and A. S. Elshall, Hierarchical Bayesian model averaging for hydrostratigraphic modeling: Uncertainty segregation and comparative evaluation, Water Resources Research, 2013. (accepted)
22. Nadiri, A.A., N. Chitsazan, F. T.-C. Tsai, and A. Asghari Moghaddam. Bayesian Artificial Intelligence Model Averaging for Hydraulic Conductivity Estimation. ASCE Journal of Hydrologic Engineering, 2013. (accepted)
23. Nadiri, A.A., E. Fijani, F. T.-C. Tsai, and A. Asghari Moghaddam. Supervised Committee Machine with Artificial Intelligence for Prediction of Fluoride Concentration, Journal of Hydroinformatics, 2013. (accepted)
24. Chamberlain, Elizabeth Laurel, Depositional Environments of Upper Miocene through Pleistocene Siliciclastic Sediments, Baton Rouge Aquifer System, Southeastern Louisiana, Master of Science Thesis, Department of Geology and Geophysics, Louisiana State University, 66p.
25. Frank Tsai, 2012, Feasibility Study of Scavenging Approach to Stop Saltwater Toward Water Wells, Louisiana State University, Baton Rouge, Louisiana, 10 pages. (USGS 104B)
26. Frank Tsai, 2013, Hydrostratigraphy Modeling of the Southern Hills Aquifer System and Faults, Louisiana State University, Baton Rouge, Louisiana, 10 pages. (USGS 104B)
27. Tsai F. T.-C. Tsai, and A. S. Elshall, A Bayesian Model Averaging Method to Characterize the Baton Rouge Aquifer System, 2012 World Environmental & Water Resources Congress, Albuquerque, NM, May 20-24, 2012
28. Tsai, F. T.-C., A. Mani, H. V. Pham, E. Beigi, A. S. Elshall, and N. Chitsazan, Characterization of Siliciclastic Aquifer-Fault System for Southeastern Louisiana, 2013 World Environmental & Water Resources Congress, Cincinnati, OH, May 19-23, 2013

29. Pham, H. V., A. S. Elshall, F. T.-C. Tsai, and L. Yan, Parallel Inverse Groundwater Modeling Using CMA-ES, 2013 World Environmental & Water Resources Congress, Cincinnati, OH, May 19-23, 2013
30. Hanor, J. S., E. L. Chamberlain and F. T.-C. Tsai, A Conceptual Model for the Evolution of the Permeability Architecture of the Baton Rouge Fault Zone, Southeastern Louisiana, 7th Annual Groundwater and Water Resources Symposia, Baton Rouge, LA, 8 May 2013.
31. Elshall, A. S., F. T.-C. Tsai and J. S. Hanor, Reconstructing Baton Rouge aquifer-fault hydrostratigraphy using indicator geostatistics, 7th Annual Groundwater and Water Resources Symposia, Baton Rouge, LA, 8 May 2013
32. Pham, H. V. and F. T.-C. Tsai, Development of groundwater model for the “1,200-foot”, “1,500-foot” and “1,700-foot” sands of the Baton Rouge area, Southeastern Louisiana, 7th Annual Groundwater and Water Resources Symposia, Baton Rouge, LA, 8 May 2013.
33. Beigi, E. and F. T.-C. Tsai, Modeling of Potential Groundwater Recharge under Climate Change of Southern Hills Aquifer System, Southeastern Louisiana and Southwestern Mississippi, 7th Annual Groundwater and Water Resources Symposia, Baton Rouge, LA, 8 May 2013
34. Beigi, E., and F. T.-C. Tsai, Climate Impact on Groundwater Recharge in Southeastern Louisiana and Southwestern Mississippi, H13B-1317 Abstract, 2012 American Geophysical Union Fall Meeting, San Francisco, CA, 3-7 December 2012.
35. Elshall, A. S., F. T.-C. Tsai, J. S. Hanor, Hydrogeophysical Data Fusion and Geostatistical Approach to Characterize Hydrogeological Structure of the Baton Rouge Aquifer System in Louisiana, H13B-1336 Abstract, 2012 American Geophysical Union Fall Meeting, San Francisco, CA, 3-7 December 2012.
36. Pham, H. V., A. S. Elshall, F. T.-C. Tsai, and L. Yan, Local Derivative-Free Parallel Computing Method for Solving the Inverse Problem in Groundwater Modeling, H21A-1164 Abstract, 2012 American Geophysical Union Fall Meeting, San Francisco, CA, 3-7 December 2012.
37. Chitsazan, N. and F. T.-C. Tsai, Hierarchical Bayesian Model Averaging for Chance Constrained Remediation Designs, H33I-1450 Abstract, 2012 American Geophysical Union Fall Meeting, San Francisco, CA, 3-7 December 2012
38. Tsai, F. T.-C., A. S. Elshall and J. S. Hanor, A Hierarchical Multi-Model Approach for Uncertainty Segregation, Prioritization and Comparative Evaluation of Competing Modeling Propositions, H43B-1326 Abstract, 2012 American Geophysical Union Fall Meeting, San Francisco, CA, 3-7 December 2012
39. Chamberlain, E. L., J. S. Hanor, and F. T.-C. Tsai, Sequence Stratigraphic Characterization of Upper Miocene through Pleistocene Siliciclastic Aquifer Sediments, Baton Rouge Area, Southeastern Louisiana Gulf Coast, H13B-1325 Abstract, 2012 American Geophysical Union Fall Meeting, San Francisco, CA, 3-7 December 2012
40. Nadiri, A. A., N. Chitsazan, F. T.-C. Tsai, and A. Asghari Moghaddam, Bayesian Model Averaging of Artificial Intelligence Models for Hydraulic Conductivity Estimation, H13B-1338 Abstract, 2012 American Geophysical Union Fall Meeting, San Francisco, CA, 3-7 December 2012
41. Fijani, E., N. Chitsazan, A. A. Nadiri, F. T.-C. Tsai, and A. Asghari Moghaddam, Hierarchical Bayesian Model Averaging for Non-Uniqueness and Uncertainty Analysis of Artificial Neural Networks, H43B-1343 Abstract, 2012 American Geophysical Union Fall Meeting, San Francisco, CA, 3-7 December 2012
42. • Frank Tsai, 2012, Feasibility Study of Scavenging Approach to Stop Saltwater Toward Water Wells, Louisiana State University, Baton Rouge, Louisiana, 10 pages. (USGS 104B)
43. Tsai, F. T.-C., and A.S. Elshall. (2011). A Hierarchical Bayesian Model Averaging Approach to Cope With Sources of Uncertainty in Conceptual Ground Water Models, World Water & Environmental Resources Congress, Palm Springs, CA, May 22-26, 2011.
44. Tsai, F. T.-C. (2011). Development of Scavenger Well Operation Model To Stop Saltwater Intrusion Toward Water Wells In The “1,500-Foot” Sand of The Baton Rouge Area, Louisiana, World Water & Environmental Resources Congress, Palm Springs, CA, May 22-26, 2011.

45. Tsai, F. T.-C. (2011). Scavenger Wells Stop Saltwater Intrusion in Baton Rouge, Louisiana, MODFLOW and More 2011, Golden, CO, June 5-8, 2011
46. Elshall, A. S., F. T.-C. Tsai, J. S. Hanor, Indicator geostatistics for reconstructing Baton Rouge aquifer-fault hydrostratigraphy (Louisiana, USA), Hydrogeology Journal, 2013. (accepted)
47. Tsai, F. T.-C. and A. S. Elshall, Hierarchical Bayesian model averaging for hydrostratigraphic modeling: Uncertainty segregation and comparative evaluation, Water Resources Research, 2013. (accepted)
48. Nadiri, A.A., N. Chitsazan, F. T.-C. Tsai, and A. Asghari Moghaddam. Bayesian Artificial Intelligence Model Averaging for Hydraulic Conductivity Estimation. ASCE Journal of Hydrologic Engineering, 2013. (accepted)
49. Nadiri, A.A., E. Fijani, F. T.-C. Tsai, and A. Asghari Moghaddam. Supervised Committee Machine with Artificial Intelligence for Prediction of Fluoride Concentration, Journal of Hydroinformatics, 2013. (accepted)
50. Chamberlain, Elizabeth Laurel, Depositional Environments of Upper Miocene through Pleistocene Siliciclastic Sediments, Baton Rouge Aquifer System, Southeastern Louisiana, Master of Science Thesis, Department of Geology and Geophysics, Louisiana State University, 66p.
51. Frank Tsai, 2012, Feasibility Study of Scavenging Approach to Stop Saltwater Toward Water Wells, Louisiana State University, Baton Rouge, Louisiana, 10 pages. (USGS 104B)
52. Frank Tsai, 2013, Hydrostratigraphy Modeling of the Southern Hills Aquifer System and Faults, Louisiana State University, Baton Rouge, Louisiana, 10 pages. (USGS 104B)
53. Tsai F. T.-C. Tsai, and A. S. Elshall, A Bayesian Model Averaging Method to Characterize the Baton Rouge Aquifer System, 2012 World Environmental & Water Resources Congress, Albuquerque, NM, May 20-24, 2012
54. Tsai, F. T.-C., A. Mani, H. V. Pham, E. Beigi, A. S. Elshall, and N. Chitsazan, Characterization of Siliciclastic Aquifer-Fault System for Southeastern Louisiana, 2013 World Environmental & Water Resources Congress, Cincinnati, OH, May 19-23, 2013
55. Pham, H. V., A. S. Elshall, F. T.-C. Tsai, and L. Yan, Parallel Inverse Groundwater Modeling Using CMA-ES, 2013 World Environmental & Water Resources Congress, Cincinnati, OH, May 19-23, 2013
56. Hanor, J. S., E. L. Chamberlain and F. T.-C. Tsai, A Conceptual Model for the Evolution of the Permeability Architecture of the Baton Rouge Fault Zone, Southeastern Louisiana, 7th Annual Groundwater and Water Resources Symposia, Baton Rouge, LA, 8 May 2013.
57. Elshall, A. S., F. T.-C. Tsai and J. S. Hanor, Reconstructing Baton Rouge aquifer-fault hydrostratigraphy using indicator geostatistics, 7th Annual Groundwater and Water Resources Symposia, Baton Rouge, LA, 8 May 2013
58. Pham, H. V. and F. T.-C. Tsai, Development of groundwater model for the “1,200-foot”, “1,500-foot” and “1,700-foot” sands of the Baton Rouge area, Southeastern Louisiana, 7th Annual Groundwater and Water Resources Symposia, Baton Rouge, LA, 8 May 2013.
59. Beigi, E. and F. T.-C. Tsai, Modeling of Potential Groundwater Recharge under Climate Change of Southern Hills Aquifer System, Southeastern Louisiana and Southwestern Mississippi, 7th Annual Groundwater and Water Resources Symposia, Baton Rouge, LA, 8 May 2013
60. Beigi, E., and F. T.-C. Tsai, Climate Impact on Groundwater Recharge in Southeastern Louisiana and Southwestern Mississippi, H13B-1317 Abstract, 2012 American Geophysical Union Fall Meeting, San Francisco, CA, 3-7 December 2012.
61. Elshall, A. S., F. T.-C. Tsai, J. S. Hanor, Hydrogeophysical Data Fusion and Geostatistical Approach to Characterize Hydrogeological Structure of the Baton Rouge Aquifer System in Louisiana, H13B-1336 Abstract, 2012 American Geophysical Union Fall Meeting, San Francisco, CA, 3-7 December 2012.
62. Pham, H. V., A. S. Elshall, F. T.-C. Tsai, and L. Yan, Local Derivative-Free Parallel Computing Method for Solving the Inverse Problem in Groundwater Modeling, H21A-1164 Abstract, 2012 American Geophysical Union Fall Meeting, San Francisco, CA, 3-7 December 2012.

63. Chitsazan, N. and F. T.-C. Tsai, Hierarchical Bayesian Model Averaging for Chance Constrained Remediation Designs, H33I-1450 Abstract, 2012 American Geophysical Union Fall Meeting, San Francisco, CA, 3-7 December 2012
64. Tsai, F. T.-C., A. S. Elshall and J. S. Hanor, A Hierarchical Multi-Model Approach for Uncertainty Segregation, Prioritization and Comparative Evaluation of Competing Modeling Propositions, H43B-1326 Abstract, 2012 American Geophysical Union Fall Meeting, San Francisco, CA, 3-7 December 2012
65. Chamberlain, E. L., J. S. Hanor, and F. T.-C. Tsai, Sequence Stratigraphic Characterization of Upper Miocene through Pleistocene Siliciclastic Aquifer Sediments, Baton Rouge Area, Southeastern Louisiana Gulf Coast, H13B-1325 Abstract, 2012 American Geophysical Union Fall Meeting, San Francisco, CA, 3-7 December 2012
66. Nadiri, A. A., N. Chitsazan, F. T.-C. Tsai, and A. Asghari Moghaddam, Bayesian Model Averaging of Artificial Intelligence Models for Hydraulic Conductivity Estimation, H13B-1338 Abstract, 2012 American Geophysical Union Fall Meeting, San Francisco, CA, 3-7 December 2012
67. Fijani, E., N. Chitsazan, A. A. Nadiri, F. T.-C. Tsai, and A. Asghari Moghaddam, Hierarchical Bayesian Model Averaging for Non-Uniqueness and Uncertainty Analysis of Artificial Neural Networks, H43B-1343 Abstract, 2012 American Geophysical Union Fall Meeting, San Francisco, CA, 3-7 December 2012
68. Chitsazan, N. and F. T.-C. Tsai. (2014). Uncertainty segregation and comparative evaluation in groundwater remediation designs: A chance-constrained hierarchical Bayesian model averaging approach, *Journal of Water Resources Planning and Management* (accepted), doi: 10.1061/(ASCE)WR.1943-5452.0000461
69. Chitsazan, N. and F. T.-C. Tsai. (2014). A Hierarchical Bayesian Model Averaging Framework for Groundwater Prediction under Uncertainty, *Groundwater* (in press), doi: doi: 10.1111/gwat.12207
70. Elshall, A.S., F. T.-C. Tsai. (2014). Constructive epistemic modeling of groundwater flow with geological architecture and boundary condition uncertainty under Bayesian paradigm, *Journal of Hydrology*. (in press) doi: 10.1016/j.jhydrol.2014.05.027
71. Beigi, E., and Tsai, F. T.-C. (2014). A GIS-based water budget framework for parallel computing high-resolution groundwater recharge in humid regions. *Journal of Hydrologic Engineering*, (in press) doi:10.1061/(ASCE)HE.1943-5584.0000993
72. Nadiri, A.A., N. Chitsazan, F. T.-C. Tsai, and A. Asghari Moghaddam. (2014). Bayesian Artificial Intelligence Model Averaging for Hydraulic Conductivity Estimation. *Journal of Hydrologic Engineering*, 19, 520-532. doi:10.1061/(ASCE)HE.1943-5584.0000824
73. Elshall, A.S., F. T.-C. Tsai, and J.S. Hanor. (2013). Indicator Geostatistics for Reconstructing Baton Rouge Aquifer-Fault Hydrostratigraphy, Louisiana, USA. *Hydrogeology Journal*, 21, 1731-1747. doi:10.1007/s10040-013-1037-5
74. Tsai, F. T.-C., and A. S. Elshall. (2013). Hierarchical Bayesian model averaging for hydrostratigraphic modeling: Uncertainty segregation and comparative evaluation. *Water Resources Research*, 49, 5520-5536. doi:10.1002/wrcr.20428
75. Nadiri, A.A., E. Fijani, F. T.-C. Tsai, and A. Asghari Moghaddam. (2013). Supervised Committee Machine with Artificial Intelligence for Prediction of Fluoride Concentration, *Journal of Hydroinformatics*, 15(4), 1474-1490. 10.2166/hydro.2013.008
76. Chamberlain, Elizabeth Laurel (2012), Depositional Environments of Upper Miocene through Pleistocene Siliciclastic Sediments, Baton Rouge Aquifer System, Southeastern Louisiana, Master of Science Thesis, Department of Geology and Geophysics, Louisiana State University, 66p.
77. Chitsazan, Nima (2014), Bayesian Saltwater Intrusion Prediction and Groundwater Remediation Design under Uncertainty, Doctor of Philosophy Dissertation, Department of Civil and Environmental Engineering, Louisiana State University
78. Frank Tsai, 2013, Hydrostratigraphy Modeling of the Southern Hills Aquifer System and Faults, Louisiana State University, Baton Rouge, Louisiana, 10 pages. (USGS 104B)

Hierarchical Multimodel Saltwater Intrusion Remediation and Sampling Designs: A BMA Tree Approach

79. Biegi, E., and F. T.-C. Tsai, 2014, Comparative Study of Climate Change Scenarios on Groundwater Recharge, World Environmental & Water Resources Congress, Portland, Oregon June 1-5, 2014.
80. Chamberlain, E. L., J. S. Hanor, and F. T.-C. Tsai, 2013, Sequence stratigraphic characterization of the Baton Rouge aquifer system, southeastern Louisiana: Gulf Coast Association of Geological Societies Transactions, v. 63, p. 125-136, 2013
81. Chitsazan, N., H. V. Pham, F. T.-C. Tsai, and J. S. Hanor, 2013, Salinization simulation for the “1200–1500–1700-foot” sands of the Baton Rouge area, southeastern Louisiana: Gulf Coast Association of Geological Societies Transactions, v. 63, p. 519-522, 2013
82. Elshall, A. S., F. T.-C. Tsai, and J. S. Hanor, Indicator geostatistical approach to reconstruct geological architecture of the Baton Rouge aquifer-fault system, Louisiana. Gulf Coast Association of Geological Societies Transactions. v. 63, p. 539-542, 2013

Problem and Research Objectives

Water use in Baton Rouge, Louisiana is approximately 171.41 million gallons per day out of which 87.4% is ground water and the rest is surface water (Sargent, 2012). Population served by public supply is 436,650. Due to excessive ground water pumping, saltwater is intruding from the saline aquifers in the south part of the Baton Rouge Fault. Thus, in the absence of any remediation measure, some of public supply water wells in East Baton Rouge Parish are under the threat of being abandoned in the near future. The project objective is to develop saltwater intrusion models to be employed for the management and remediation of the ground water resources for the study area shown in Figure 1. The study area is approximately 500 km².

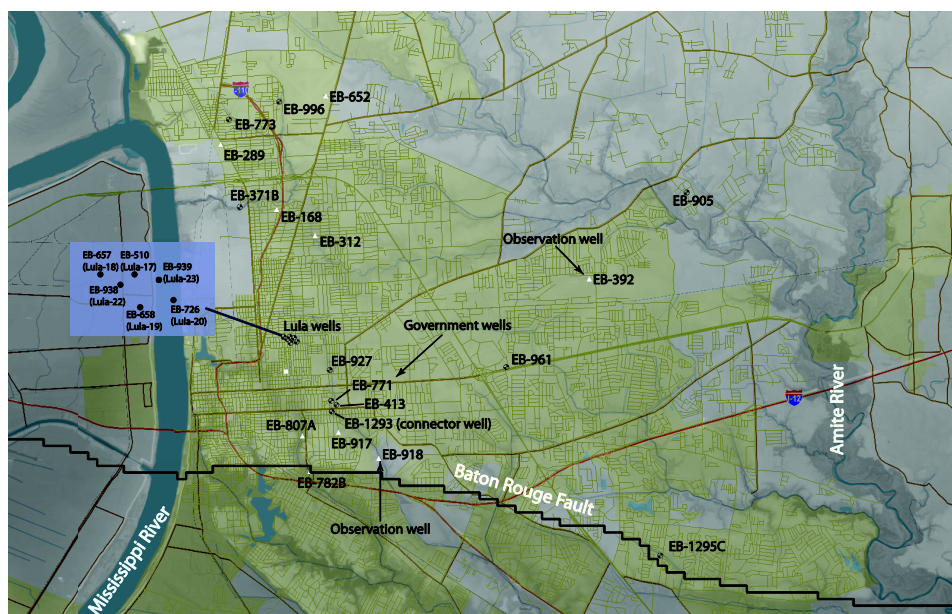


Figure 1: The map of the study area. Circles are pumping wells. White triangles are USGS water wells. All wells in the map were screened at the “1,500-foot” sand.

Due to limited amount of data and since model uncertainty always exists, multiple models are usually developed. Model selection, model elimination, model reduction, and model discrimination are commonly used to select the best model. It is clear that modeling uncertainty is always underestimated if only the best model is used. One would ask why only the best model is used afterwards when so many efforts have been devoted to calibrating many models. This certainly wastes valuable resources and important information from other good models. Hierarchical Bayesian model averaging (HBMA) (Chitsazan and Tsai, 2012; Tsai and Elshall, 2013) best utilize all possible models for model prediction and application under Bayesian statistical framework. HBMA presents several advantages over model selection: (1) Information from all possible models is used based on their model importance (model weights). Calibration efforts are not wasted. (2) The model importance is based on the evidence of data, which avoids over-confidence in the best model that does not have a dominant model weight. And (3) model structure uncertainty is increased and is better presented than that by using a single model. Moreover, HBMA is able to distinguish model uncertainty arising from individual models and

between models. HBMA is able to identify unfavorable models even though they may present small prediction uncertainty.

In this study, the HBMA is used to predict chloride concentration and estimate prediction uncertainty for the “1,500-foot” sand in the Baton Rouge aquifer system. The HBMA is applied to analyze the conceptual model structure uncertainty arising from the different competing model propositions for chloride concentration predictions at the USGS water quality wells.

Methodology

Hierarchical Bayesian Model Averaging (HBMA)

To cope with different sources of uncertainty in groundwater flow and mass transport models, a hierarchical Bayesian model averaging is developed (Tsai and Elshall, 2013). Consider $M_{\underbrace{(ij\dots lm)}_p} \in \mathbf{M}_p$ a model at level p . The subscript $\underbrace{(ij\dots lm)}_p$ locates the model

hierarchically top down from the first level, to the second level and so forth to reach to level p . For example, $M_{(i)} \in \mathbf{M}_1$ is model i at level 1, $M_{(ij)} \in \mathbf{M}_2$ is model j at level 2, which is a child model to parent model i at level 1. $M_{(ijk)} \in \mathbf{M}_3$ is model k at level 3, which is a child model to the parent model j at level 2 and the grandparent model of model i at level 1. From bottom up, parent models \mathbf{M}_{p-1} at level $p-1$ is composed of the child models \mathbf{M}_p at level p . Models \mathbf{M}_{p-2} at level $p-2$ are composed of models \mathbf{M}_{p-1} at level $p-1$ and so forth until the Hierarch BMA model M_0 is reached.

Consider base models at level p . According to the law of total probability, the posterior probability for predicted quantity Δ given data \mathbf{D} is

$$\Pr(\Delta | \mathbf{D}) = E_{\mathbf{M}_1} E_{\mathbf{M}_2} \dots E_{\mathbf{M}_p} \left[\Pr(\Delta | \mathbf{D}, \mathbf{M}_p) \right], \quad (1)$$

where $E_{\mathbf{M}_p}$ is the expectation operator with respect to models \mathbf{M}_p at level p . $\Pr(\Delta | \mathbf{D}, \mathbf{M}_p)$ is the posterior probability of predicted quantity Δ given data \mathbf{D} and models \mathbf{M}_p at level p . The expectation $E_{\mathbf{M}_p} [\Pr(\Delta | \mathbf{D}, \mathbf{M}_p)]$ is posterior probability averaging at level p . That is

$$E_{\mathbf{M}_p} \left[\Pr(\Delta | \mathbf{D}, \mathbf{M}_p) \right] = \sum_m \Pr \left(\Delta | \mathbf{D}, M_{\underbrace{(ij\dots lm)}_p} \right) \Pr \left(M_{\underbrace{(ij\dots lm)}_p} | \mathbf{D}, M_{\underbrace{(ij\dots l)}_{p-1}} \right). \quad (2)$$

where $\Pr \left(\Delta | \mathbf{D}, M_{\underbrace{(ij\dots lm)}_p} \right) = \Pr(\Delta | \mathbf{D}, \mathbf{M}_p)$.

$\Pr \left(M_{\underbrace{(ij\dots lm)}_p} | \mathbf{D}, M_{\underbrace{(ij\dots l)}_{p-1}} \right) = \Pr(\mathbf{M}_p | \mathbf{D}, \mathbf{M}_{p-1})$ is the conditional posterior model probability of

model $M_{\underbrace{(ij\dots lm)}_p}$ at level p under model $M_{\underbrace{(ij\dots l)}_{p-1}}$ at level $p-1$. $\Pr(\mathbf{M}_p | \mathbf{D}, \mathbf{M}_{p-1})$ also represents the conditional model weights and will be used to develop a BMA tree of model weights. Note that model $M_{(ij\dots lm)}$ is a child model under the parent model $M_{(ij\dots l)}$ because both have the same subscript for the first $p-1$ levels. Equation (2) is the Bayesian model averaging (BMA) at level p , which can be written as

$$\Pr(\Delta | \mathbf{D}, \mathbf{M}_{p-1}) = E_{\mathbf{M}_p} \left[\Pr(\Delta | \mathbf{D}, \mathbf{M}_p) \right]. \quad (3)$$

According to equations (1) and (3), one can derive the posterior probability of prediction using BMA over models at any level, say level n:

$$\Pr(\Delta | \mathbf{D}, \mathbf{M}_n) = E_{\mathbf{M}_{n+1}} E_{\mathbf{M}_{n+2}} \dots E_{\mathbf{M}_p} \left[\Pr(\Delta | \mathbf{D}, \mathbf{M}_p) \right]. \quad (4)$$

Based on equation (4), the law of total expectation and the law of total variance, the prediction mean, within-model variance, between model variance and total variance can be derived at level n.

The hierarch BMA model is the usual BMA model (Hoeting et al., 1999), which is based on equation (1). The hierarch model obtains model averaging results and prediction variances using all base models.

In this study, Δ is the concentration and \mathbf{D} is groundwater head and concentration data used to calibrate groundwater flow and transport models.

Principal Findings and Significance

(1) Saltwater intrusion modeling in the “1,500-foot” sand of the Baton Rouge area

We develop a two-dimensional groundwater flow and mass transport model to predict the saltwater intrusion in the “1,500-foot” sand of the Baton Rouge area. The study area, shown in Figure 1, includes the east-west trending Baton Rouge fault (see Figure 1). The saltwater intrusion model in this report is based on Tsai (2010, 2011). The simulation period is from 1/1/1990 to 12/31/2029 which is divided in calibration part from 1/1/1990 to 1/1/2005 and prediction part from 1/1/2005 to 12/31/2029. The initial groundwater head and the initial chloride concentration are obtained from Tsai (2011). The groundwater model uses the time-varied constant boundary condition for all the boundaries. The mass transport model uses constant concentration in the south boundary. The concentrations in the other boundaries are calculated by the transport simulation model in each time step. The major production wells are Lula pump station and Government Street pump station, which are located north of the Baton Rouge fault. The average pumping rate from Lula pump station is 7.03 million gallons per day and at Government Street pump station is 1.59 million gallons per day. We use MODFLOW (Harbaugh, 2005) and MT3DMS (Zheng and Wang, 1999) to simulate the groundwater flow and mass transport from 1/1/1990 to 12/31/2029. We use 706 head observations from 1/1/1990 to 1/1/2005 at the USGS observation wells shown in Figure 1 to calibrate the model. Then, we develop the prediction models to predict salt water intrusion from 1/1/2005 to 12/31/2029.

(2) Sources of uncertainty and multiple models

We analyze four sources of uncertainty in a hierarchical order in the flow and transport models. They are (1) boundary condition uncertainty, (2) grain-size method uncertainty in determining point-wise hydraulic conductivity, (3) variogram model uncertainty in kriging hydraulic conductivity distribution, and (4) fault permeability architecture uncertainty. To address these sources of uncertainty, 5 boundary condition propositions, three grain-size methods (Kozeny-Carman, Slitcher, and Terzaghi methods), three variogram models (exponential, Gaussian, and spherical), and 3 fault permeability architectures are proposed. This results in $5 \times 3 \times 3 \times 4 = 180$ saltwater intrusion simulation models at the base level of the BMA tree.

In order to track a model in the BMA tree, we use the letter “B” subscribed with percentage of change of boundary head values in the determined boundary condition, the first letter of the grain-size methods, the first letter of the variogram model and the number of fault permeability segments in a hierarchical way to denote a model. For example “B₀KG3” denotes a base model in level 4 that consider no change in the determined boundary condition, Kozeny-Carman method, the Gaussian variogram and three-segment fault permeability architecture. “B₀KG” is a BMA model at level 3 that averages base models with different fault permeability architectures given “B₀” boundary condition, “K” grain-sized method and “G” variogram model propositions. “B₀K” is a BMA model at level 2 that averages level-3 BMA models with different grain-size method propositions given “B₀” boundary condition proposition. “B₀” is a BMA model at level 1 that averages level-2 BMA models with different variogram model propositions given “B₀” boundary condition and “K” grain-sized method propositions.

(3) BMA Tree of model weights

Figure 2 shows the BMA tree of model weights in parentheses and conditional model weights. The model weights reflect the comparative importance of all the competitive modeling propositions in one level. The conditional model weights represent the relative importance of the different propositions under the same parent models. The base level of the BMA tree corresponds to different fault permeability segments. The simulation models using homogeneous fault permeability can be discarded because they provide very poor fitting to the observation data and are not shown in the BMA tree.

At the base level, the best base model is B₀KG3 with the model weight 20.41%. At the third level, the BMA models are developed by averaging concentration predictions from their child base models that use different fault permeability architectures. The “B₀KG” is the best model with model weight 38.93% the second best model is the “B₀KS” with model weight 28.75%. The relative model weights show that the ranking of the variogram models is the same under both “B₀K” and “B₊₁₀K” models. The Gaussian model is a better proposition than the spherical and exponential models to determine the hydraulic conductivity distribution.

At the second level, BMA models are developed by averaging concentration predictions from their child BMA models that use different variogram models for hydraulic conductivity estimation. As shown in Figure 2, since Terzaghi and Slitcher methods have significantly worse fit to the observation data, only Kozeny-Carman method are remained at the second level. The “B₀K” model weight is 78.64% and the “B₊₁₀K” model weight is 21.36%. Their conditional model weights are 100% under their parent model.

At the first level, BMA models are developed by averaging concentration predictions by their child BMA models that use different grain-size methods. However, from previous analysis, we found that only Kozeny-Carman method was left to be used. At this level the determined boundary condition (B₀) is dominantly the best model with the model weight 78.64% and B₊₁₀ is the second best model with model weight 21.36%. Other boundary condition propositions are discarded because of poor fitting to the observation data.

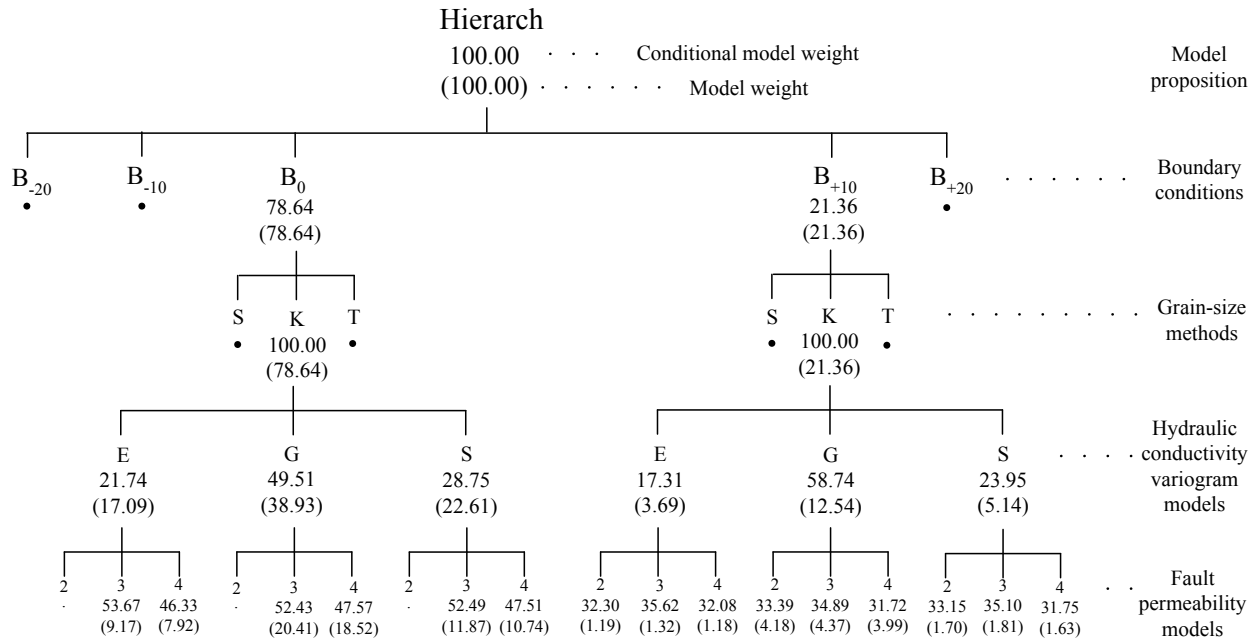
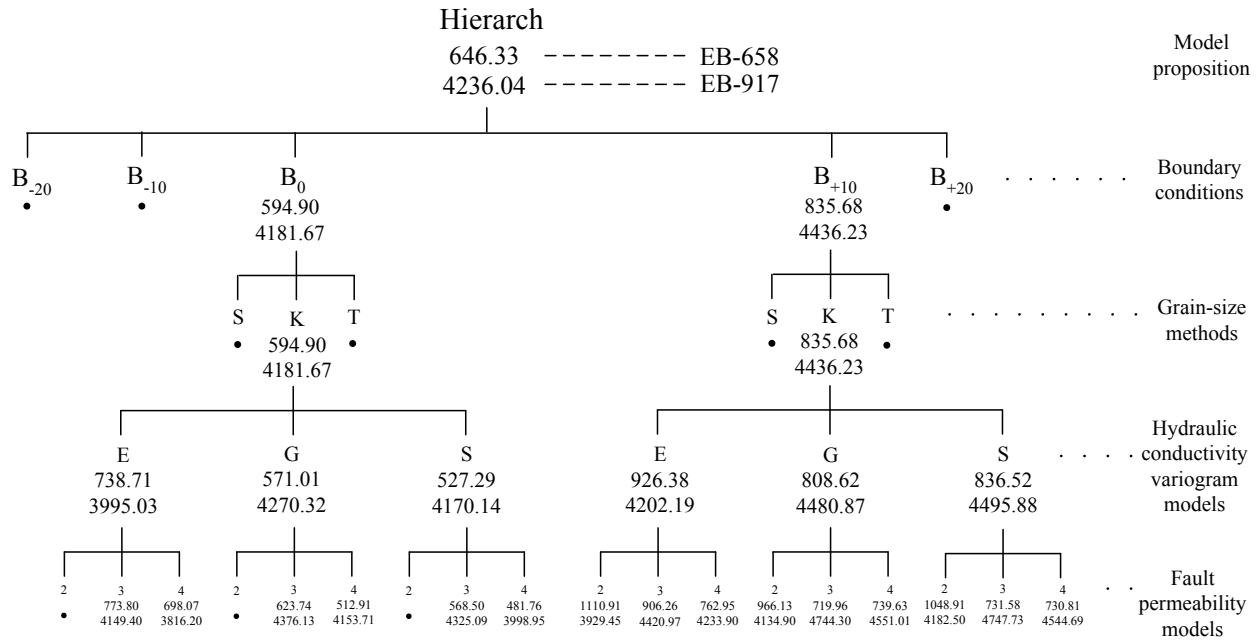


Figure 2: BMA tree of model weights and conditional model weghits.

(4) BMA tree of mean concentration predictions

The BMA tree of mean concentration predictions for the EB-658 and the EB-917 on 12/31/2029 is shown in Figure 3. The predicted mean concentration at EB-658 at the base level is between 481.76 mg/L and 1110.91 mg/L and. The predicted mean concentration at EB-917 at the base level is between 3816.20 mg/L and 4747.73 mg/L. The mean concentration prediction range becomes narrower while going up to upper layers because of the nature of averaging and the reduction in the number of models. At the level 3 the mean concentration range at EB-658 is between 527.29 mg/L and 926.38 mg/L and the mean concentration range at EB-917 is between 3995.03 mg/L and 4495.88 mg/L. At the level 2 and level 3, the concentration prediction range for EB-658 is between 594.90 mg/L and 835.68 mg/L and for EB-917 is between 4181 mg/L and 4436.23 mg/L. The hierarch BMA model predicts mean concentration at EB-658 and EB-917 is 646.33 mg/L and 4236.04 mg/L. It was found that all of the models with 3-segment fault proposition predict higher mean concentration at EB-917 than the models with 2-segment or 4-segment fault proposition.

The BMA tree of mean predictions shown in Figure 3 provides an understanding of mean prediction variability over the accumulation of sources of uncertainty, which is not possible to know via the traditional BMA method.



PR

Figure 3: BMA tree of mean concentration predictions (mg/L) at the EB-658 and EB-917 at the 12/31/2029.

(5) Temporal predictions and variances

Figure 4 shows the EB-917 concentration predictions and the one standard deviation bound using models at the different levels for the prediction period. All of the models predict the increasing concentration at EB-917. As shown in Figure 4, none of the USGS chloride data is inside the one standard deviation bound of the B_0KG3 base model and B_0KG model. Two chloride data are in one standard deviation bound of the B_0K and B_0 models and all chloride data are in the one standard deviation bound of the hierarchy model.

According to Figure 4, it is clear to see that prediction variance caused by uncertain model parameters is much smaller than that caused by different model propositions. Moreover, the prediction variances at all levels start to increase at the beginning of time and then decrease. This behavior is reasonable because at early time all models predict similar low concentration at EB-917. Therefore the prediction variances are small. High prediction variances occur due to predicting concentration quite differently by different models. At later time all models start to predict similar high concentration at EB-917. Therefore, prediction variance decreases. The hierarchy model has much higher prediction variance comparing to the B_0 model is because it includes high prediction variance from the B_{+10} model.

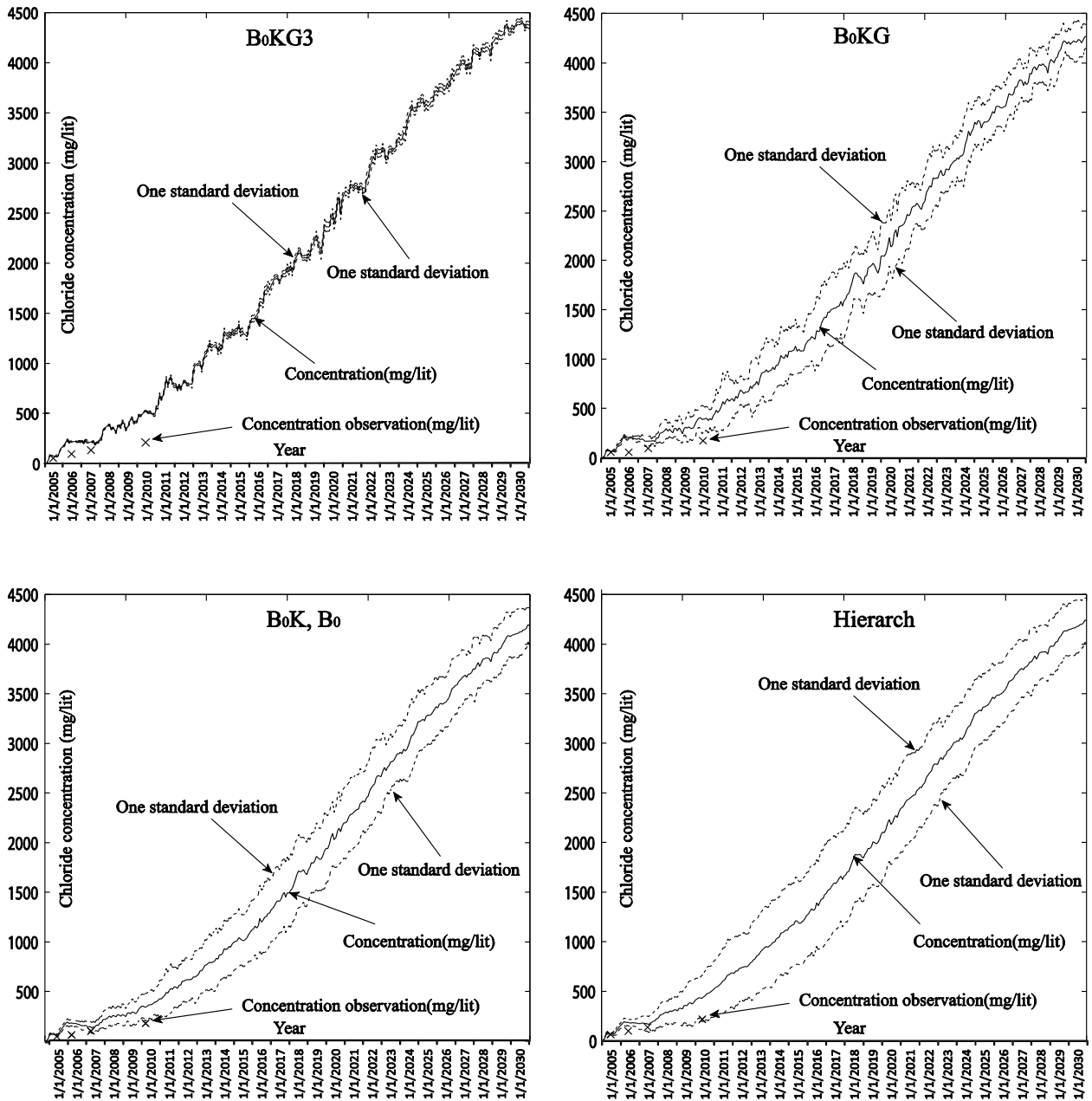


Figure 4: One standard deviation error bound of predicted concentration at EB-917 from 1/1/2005 to 12/31/2029. Crosses are USGS chloride data.

References

Chitsazan, N. and F. T.-C. Tsai, Hierarchical Bayesian model averaging for chance constrained remediation designs, H33I-1450 Abstract, 2012 American Geophysical Union Fall Meeting, San Francisco, CA, 3-7 December 2012.

Harbaugh, A.W. 2005. MODFLOW-2005: the U.S. Geological Survey modular ground-water model-The ground-water flow process: U.S. Geological Survey Techniques and Methods 6-A16.

- Hoeting, J.A., D. Madigan, A.E. Raftery, and C.T. Volinsky. 1999. Bayesian model averaging: A tutorial. *Statistical Science*, 14(4), 382-401.
- Sargent, B.P. 2012. Water use in Louisiana, 2010, Louisiana Department of Transportation and Development, Water Resources Special Report No. 17 (Revised).
- Tsai, F.T.-C. 2010. Bayesian model averaging assessment on groundwater management under model structure uncertainty. *Stochastic Environmental Research and Risk Assessment* 24(6), 845-861.
- Tsai, F.T.-C. 2011. Scavenger well operation model to assist BRWC to identify cost-effective approaches to stop saltwater intrusion toward the BRWC water wells in the “1,500-foot” sand of the Baton Rouge area. Technical report to Baton Rouge Water Company and Capital Area Groundwater Conservation Commission, Louisiana.
- Tsai, F.T.-C. and A. S. Elshall. 2013. Hierarchical Bayesian model averaging for hydrostratigraphic modeling: Uncertainty segregation and comparative evaluation, *Water Resources Research*, 2013. (accepted)
- Zheng, C. and P.P. Wang. 1999. MT3DMS—A modular three-dimensional multispecies transport model for simulation of advection, dispersion and chemical reactions of contaminants in ground-water systems; documentation and user’s guide: Jacksonville, Fla., U.S. Army Corps of Engineers Contract Report SERDP-99-1, 221p.

6. Student Support

- Nima Chitsazan, PhD student
- Ehsan Beigi, PhD student
- Ahmed Elshall, PhD student
- Elizabeth L. Chamberlain, MS student

Hydrostratigraphy Modeling of the Southern Hills Aquifer System

Basic Information

Title:	Hydrostratigraphy Modeling of the Southern Hills Aquifer System
Project Number:	2013LA91B
Start Date:	3/1/2013
End Date:	2/28/2014
Funding Source:	104B
Congressional District:	5th
Research Category:	Ground-water Flow and Transport
Focus Category:	Groundwater, Solute Transport, Methods
Descriptors:	
Principal Investigators:	Frank Tsai

Publications

1. • Elshall, A.S., F. T.-C. Tsai, and J.S. Hanor. (2013). Indicator Geostatistics for Reconstructing Baton Rouge Aquifer-Fault Hydrostratigraphy, Louisiana, USA. *Hydrogeology Journal*, 21, 1731-1747. doi:10.1007/s10040-013-1037-5
2. Frank Tsai and Jeffrey Hanor, 2013, Hierarchical Multimodel Saltwater Intrusion Remediation and Sampling Designs: A BMA Tree Approach, Louisiana Water Resources Research Institute, Louisiana State University, Baton Rouge, Louisiana, 10 pages. (USGS 104G)
3. Frank Tsai, 2013, Hydrostratigraphy Modeling of the Southern Hills Aquifer System and Faults, Louisiana Water Resources Research Institute, Louisiana State University, Baton Rouge, Louisiana, 10 pages. (USGS 104B)
4. Elshall, A. S., F. T.-C. Tsai, and J. S. Hanor, Indicator geostatistical approach to reconstruct geological architecture of the Baton Rouge aquifer-fault system, Louisiana. *Gulf Coast Association of Geological Societies Transactions*. v. 63, p. 539-542, 2013

SYNOPSIS

Problem and Research Objectives

The Southern Hills aquifer system is located in southeastern Louisiana and southwestern Mississippi shown in Figure 1. The area covers 32,678 km², ranging from latitude 30.15 to 32.56 degree and longitude from -91.81 to -89.56 degree. It includes 14 counties of Mississippi and 10 parishes of Louisiana. The area has an average slope of 11% with an elevation varying from -2 m to 172 m above mean sea level.

Figure 1: The extent of the Southern Hills aquifer system.

The lithology of the Southern Hills aquifer system is comprised of a series of sandy gravel to clayey formations that generally dip south towards the Gulf of Mexico. The surficial geology shows formations from early Miocene at the north and northwest to Pleistocene and Holocene extending from northeast to south of the aquifer system (Dicken et al. 2005). The Miocene deposits consist of Catahoula, Pascagoula, and Hattiesburg formations, the Pleistocene deposits include Citronelle and Terraces formations, and the Holocene deposits account for Mississippi River and other major stream alluvium (Buono 1983). Southeastern Louisiana also contains several east-west trending listric geologic faults (McCulloh and Heinrich 2012), which limit southward groundwater flow through the faults.



Groundwater recharge through the outcrops in southwestern Mississippi provides an important freshwater source to the deep aquifers in southeastern Louisiana. The U.S. Environmental Protection Agency (USEPA) designates the Southern Hills aquifer system as one of the sole source aquifers (SSAs), which is the only source of potable water consumed in the area overlying the aquifers and has no substitute drinking water source(s). The SSA protection program secures the Southern Hills aquifer system in order to ensure the strictest protection of the local groundwater resources from contamination, under the section 1424 of Public Law 93-523, the Safe Drinking Water Act of 1974 (US Congress 1996).

Saltwater intrusion, droughts, climate change, groundwater shortage, and potential groundwater contamination by hydraulic fracturing activities in the Tuscaloosa Marine Shale (TMS) prompt the need to study the groundwater resource in the Southern Hills aquifer system in Louisiana. To do so, the objectives of this project are to develop techniques to construct the hydrostratigraphy for the Southern Hills aquifer system with a focus on the aquifer system in the Baton Rouge area

and to convert the constructed hydrostratigraphy into the USGS MODFLOW computational grid for future groundwater flow simulation.

Methodology

(1) Hydrostratigraphy modeling

This study applies the indicator geostatistical method (Elshall et al. 2013) to the wireline well logs to construct three-dimensional geological architectures. Consider that the indicator function $\{I(\mathbf{x}, \nu) : \mathbf{x} \in \text{study area}\}$ is a random function with the indicator random variable ν describing the spatial extent of sand or clay facies. For a given sand-clay cutoff α , the random function of the indicator random variable ν for sand facies and clay facies is defined as

$$I(\mathbf{x}, \nu) = \begin{cases} 1 & \nu \in \text{Sand}, \nu(\mathbf{x}) \geq \alpha \\ 0 & \nu \in \text{Clay}, \nu(\mathbf{x}) < \alpha \end{cases} \quad (1)$$

From equation (1) the indicator outcome (one or zero) indicates the presence of sand facies or clay facies, respectively. The indicator variogram has the same definition as the normal variogram except that the real random function is replaced by the indicator random function $I(\mathbf{x}, \nu)$. To calculate the expected value $\nu^*(\mathbf{x}_0)$ at location \mathbf{x}_0 , the generalized parameterization (GP) method (Tsai and Yeh 2004, Tsai 2006) is adopted as

$$\nu^*(\mathbf{x}_0) = I(\mathbf{x}_k) + \sum_{i=1}^N \lambda_i [I(\mathbf{x}_i) - I(\mathbf{x}_k)] \beta_i \quad (2)$$

where N is the number of wireline well logs, $I(\mathbf{x}_i)$ is the indicator data, λ_i is the indicator kriging weight, and β_i is the data weighting coefficient for a data point of a well log at location \mathbf{x}_i . $I(\mathbf{x}_k)$ is indicator data for a zone defined by a well log at location \mathbf{x}_k . Equation (2) shows

that the GP estimate is the same as the indicator kriging (IK) estimate $\nu^*(\mathbf{x}_0) = \sum_{i=1}^N \lambda_i I(\mathbf{x}_i)$ if

$\forall \beta_i = 1$ and is the same as the indicator zonation (IZ) estimate $\nu^*(\mathbf{x}_0) = I(\mathbf{x}_k)$ if $\forall \beta_i = 0$. For

$0 < \beta_i < 1$, the GP estimate is between the IK estimate and IZ estimate. Elshall et al. (2013) suggests an inverse method to estimate the β_i values.

(2) MODFLOW grid generation

The USGS MODFLOW (Harbaugh 2005) is widely used in the hydrogeological and groundwater communities, in which the groundwater flow is simulated using a block-centered finite-difference method. Using the structured grid, a MODFLOW grid requires that all computational layers must be continuous throughout the model domain. This requirement creates difficulties in generating MODFLOW grids for complex hydrostratigraphic architectures including unconformed sand and clay sequences, isolated sands, discontinuity, varying thicknesses, complex interconnections, pinch-outs and geological faults. An accurate conversion of hydrostratigraphic architectures into the MODFLOW grids is an important step to reduce model structure errors in groundwater models and improve model prediction results.

Due to a lack of better grid generation techniques, complex hydrostratigraphic architectures are often overly simplified into several MODFLOW layers or into a uniform layer thickness. These simplifications significantly alter the original geological information. Unreasonable sediment thickness is often offset by adjusting hydraulic conductivity and other model parameters in the model calibration procedure. As a consequence, the groundwater flow regimes are inaccurately modeled by unrealistic aquifer parameters and structures.

In this study, we develop a technique through the following three steps to generate a MODFLOW grid that matches a complex faulted hydrostratigraphic architecture. The technique is applied to develop the MODFLOW grid for the Baton Rouge aquifer system, southeastern Louisiana. The aquifer system includes the Baton Rouge fault and the Denham Springs-Scotlandville fault. Using the hydrostratigraphic modeling technique in Elshall et al. (2013), the complex faulted hydrostratigraphic architecture is constructed by more than 500 well logs. Specifically, we generate a MODFLOW grid for the sequence of the “1,200-foot” sand, the “1,500-foot” sand, the “1,700-foot” sand, and the “2,000-foot” sand for the saltwater intrusion study in this area.

Step 1: Eliminate thin sand and thin clay

To avoid an overwhelming number of computation layers in MODFLOW, it is recommended to eliminate thin sand and thin clay in each vertical column of the hydrostratigraphic grid before generating the MODFLOW grid. Given a criterion of the minimum thickness to define thin sand and thin clay, thin sand in thick clay or thin clay in thick sand are eliminated. For a sequence of thin sand and thin clay, eliminate sand or clay, whichever has total thickness less than 50% in the sequence. After cleaning up thin sand and thin clay, bed boundaries of each vertical column are assigned indices as basic information to form MODFLOW layer boundaries. A bed boundary is an interface where sediment material changes. Bed boundaries naturally form the boundaries of MODFLOW layers.

Step 2: Project neighboring bed boundaries

To account for the continuity of MODFLOW layers from neighboring columns, additional bed boundaries are added to a vertical column by projecting the bed boundaries of its four adjacent vertical columns to the column. This is an important step in order to preserve the continuity of flow pathways, especially through geological faults, pinch-out areas, or narrow connections between thick sands. A new bed boundary may be deleted if the thickness between two consecutive bed boundaries is less than a thickness threshold. The smaller the thickness threshold is, the more the bed boundaries are added to vertical columns, which increases MODFLOW layers.

Step 3: Generate MODFLOW grid

From Step 2 the minimum number of MODFLOW layers can be determined. Given a number of MODFLOW layers, this study introduces a “ruler” algorithm to assign MODFLOW layer indices to each vertical column. Again, the layer boundaries are required to match the bed boundaries. The start and the end of the ruler match the top and the bottom boundaries of a vertical column, respectively. The number of major ticks in the ruler represents the number of MODFLOW layers. The number of layers up to a bed boundary for a vertical column is obtained by comparing its bed boundary location to the ruler. For example, a bed boundary located between 0

and 1.5 in the ruler indicates one layer up to the bed boundary, between 1.5 and 2.5 indicates two layers up to the bed boundary, between 2.5 and 3.5 indicates three layers up to the bed boundary, and so forth. When the thickness between consecutive bed boundaries is small, the ruler algorithm is likely to assign two or more bed boundaries with the same number of layers up to their bed boundaries. In this case, the ruler algorithm will adjust the numbers to make sure that each bed boundary has a distinct layer index. In the last step, equal thickness of layers is given to segments that need to be divided into two or more layers based on the final assignment of the layer indices to the bed boundaries.

Principal Findings and Significance

(1) Geological architecture

We have collected and analyzed 1256 wireline well logs in southeastern Louisiana from the Louisiana Department of Natural Resources (LaDNR), the U.S. Geological Louisiana (USGS) Water Science Center, and the Louisiana Geological Survey (LGS). The location of the well logs is shown in Figure 2. Most of the well logs are in the East Baton Rouge Parish because groundwater is heavily pumped in this parish.

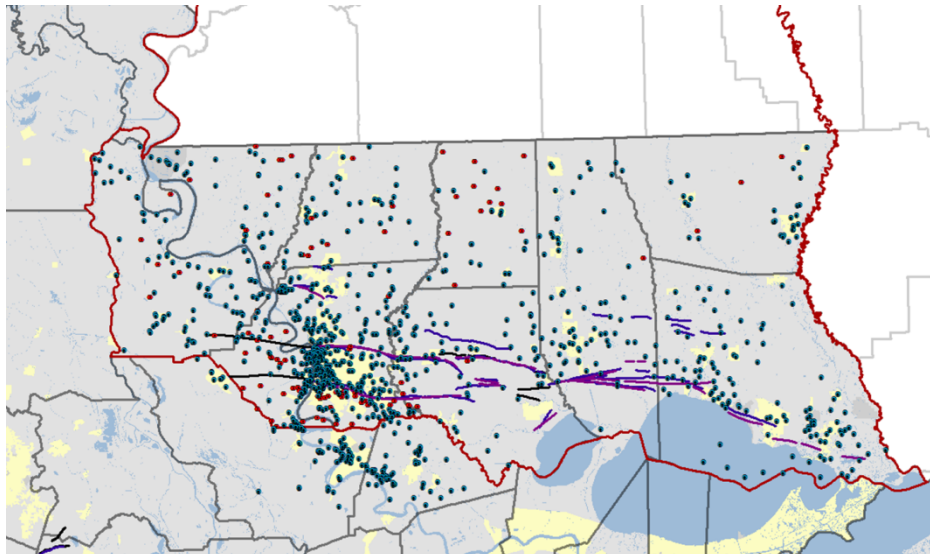


Figure 2: Location of the wireline well logs in southeastern Louisiana being analyzed for hydrostratigraphy construction. Blue circles are water well logs and red hexagons are oil/gas well logs. The blue lines are geological faults.

We analyze each well log to determine sand and clay. In general, shallow electrical resistivity (e.g., short-normal resistivity, medium induction resistivity, etc.) of 20 ohm-m is a good threshold for water-well logs to identify sand units for the freshwater formations in southeastern Louisiana. When salty water is present instead, the spontaneous-potential response helps to identify sand units. When available, the gamma ray response is used as a guide along with resistivity and spontaneous potential to identify sand units. For example, in Figure 3 the saline sands are identified in well log EB-783 located at the south of the Baton Rouge fault using SP and resistivity. For a saline sand, the SP response is pronounced and the long normal resistivity is less than the short normal resistivity. Also, the presence of salt water can be seen at the bottom of the sand in the depth of 2200 feet. Freshwater sands are identified in well log EB-1317 (south of

the Baton Rouge fault) and WBR-128 (south of the Baton Rouge fault) based on resistivity. SP is not pronouncing in these two well logs. Low gamma ray in EB-1317 correlates sand units.

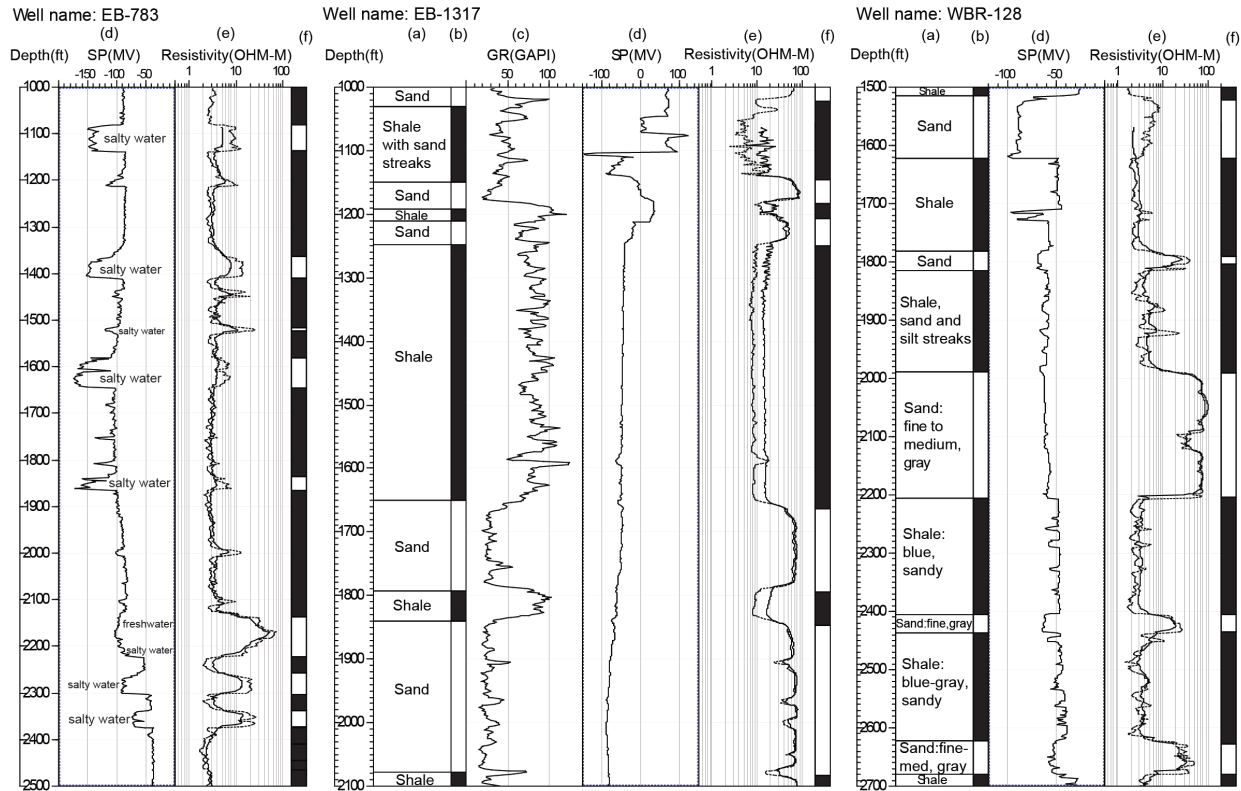


Figure 3: Wells logs for water well EB-1317, north of the Baton Rouge fault, and water wells EB-783 and WRB-128, south of the Baton Rouge fault. Column index is as follows: (a) drillers' log, (b) binary interpretation of drillers' log (white for sand and black for clay), (c) gamma ray (GR), (d) spontaneous potential (SP), (e) short normal resistivity (dotted line) and long normal resistivity (solid line), and (f) binary interpretation of electric log (white for sand and black for clay) (Elshall et al. 2013)

Using the technique in Elshall et al (2013), the geological architecture of the Southern Hills aquifer system in southeastern Louisiana was constructed as shown in Figure 4. There are many freshwater sands underneath southeastern Louisiana. Figure 5 shows the names of the sands and their depth in the Baton Rouge area.

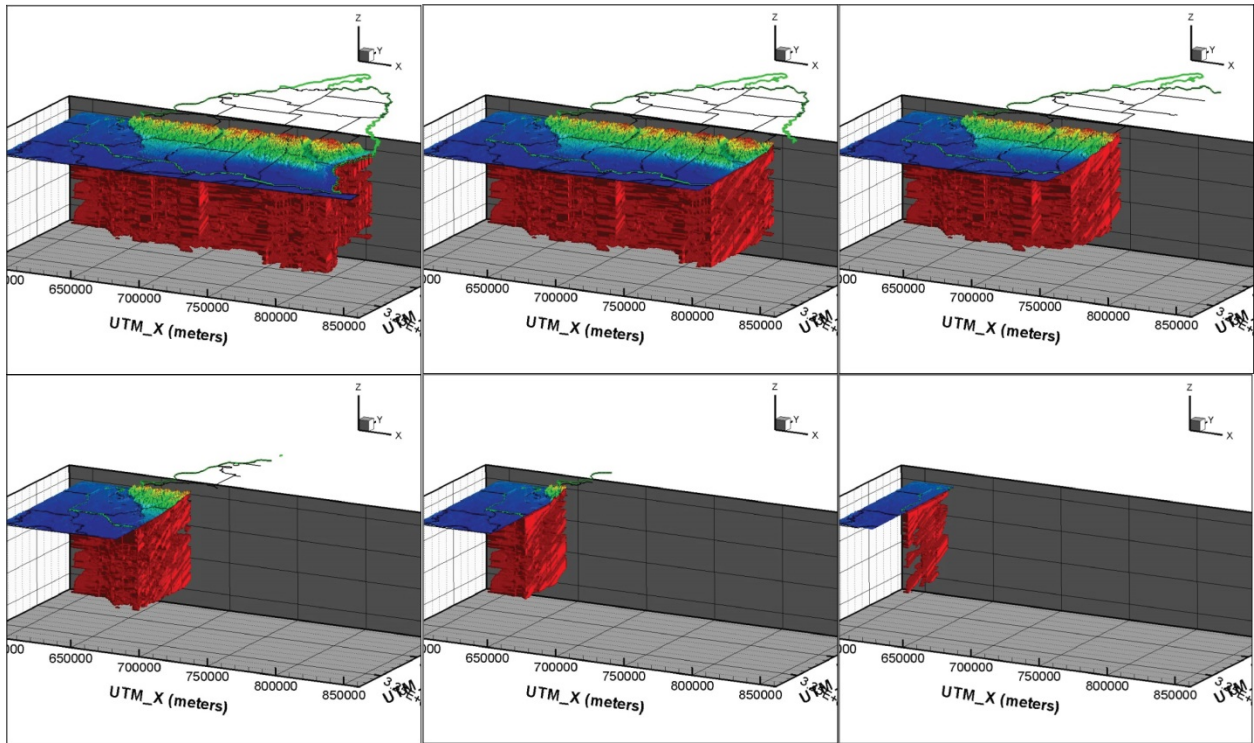


Figure 4: Geological architecture of the Southern Hills aquifer system in southeastern Louisiana

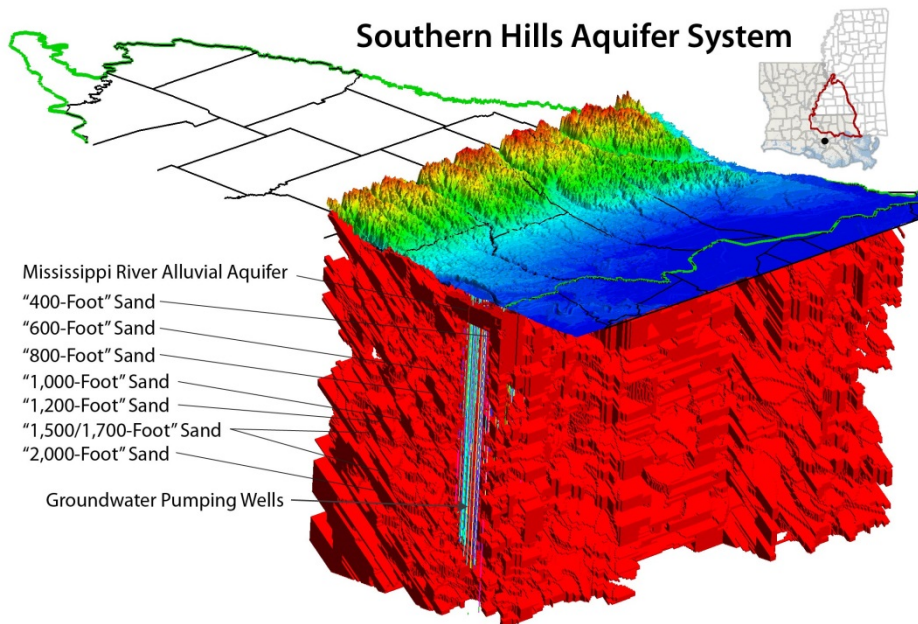


Figure 5: Geological architecture of the Southern Hills aquifer system in the Baton Rouge area

(2) MODFLOW Grid Generation

Using the proposed methodology, we convert the geological architectures of the “1,200-foot” sand, the “1,500-foot” sand, the “1,700-foot” sand, and the “2,000-foot” sand in Figure 5 into a MODFLOW grid. Figure 6 shows the hydrostratigraphy model area.

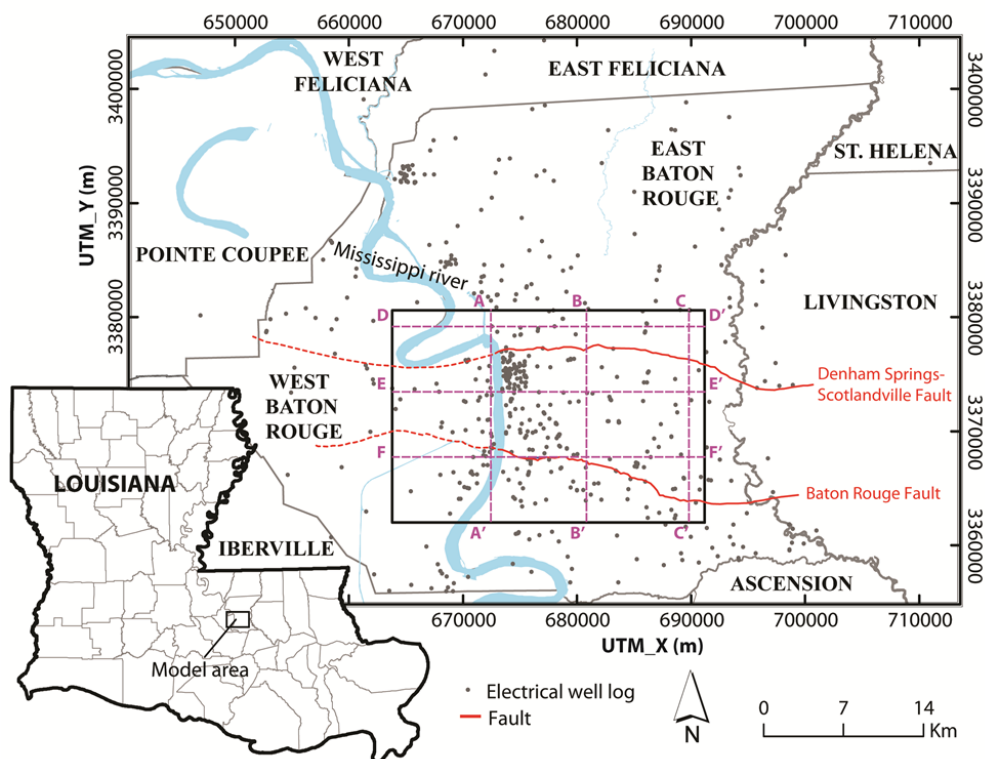


Figure 6: Map of the hydrostratigraphy model area (the box) and the location of the well logs. The solid red lines are the fault lines identified by the surface expression. The dashed red lines are the approximation surface locations of the faults.

Before eliminating thin sand and thin clay, the number of sand and clay segments in each vertical column ranges from 4 to 53, indicating at least 53 layers needed for constructing a MODFLOW grid. By eliminating sand and clay segments less than 10 ft (3.05 m) thick, the number of sand and clay segments in each vertical column is significantly reduced and ranges from 3 to 26. The second step is to consider continuity of layers by projecting the bed boundaries of four adjacent vertical columns to their respective column. After the bed boundary projection, the number of segments in vertical columns increases and ranges from 5 to 80.

In the final step, we use the processed hydrostratigraphic architecture to generate the MODFLOW grid. Figure 7 shows a grid of 76 layers, which accurately matches the complex hydrostratigraphic architecture and preserves the layer continuity. The layer thickness ranges from 3.05 m to 13.4 m. The average thickness of the layers is 5.2 meters. The “1,200-foot”, the “1,500-foot”, and the “1,700-foot” sands are from layer 6 to layer 46. The “2,000-foot” sand is from layer 47 to layer 76.

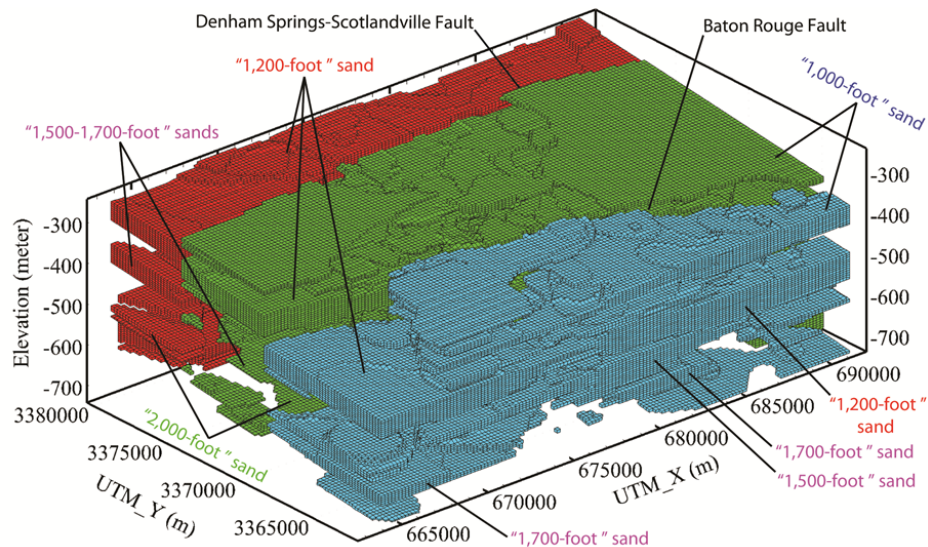


Figure 7. A three-dimensional MODFLOW grid for the “1,200-foot” sand, the “1,500-foot” sand, the “1,700-foot” sand, and the “2,000-foot” sand. Clay is blanked. The vertical exaggeration is 20 times.

Flexibility of the grid generator

Different complex three-dimensional MODFLOW grids similar to Figure 8 can be automatically regenerated using: (1) different criteria to eliminate thin sand and thin clay, (2) different thickness thresholds to delete new bed boundaries, and (3) different number of layers. Since hydrostratigraphic architectures usually carry material indices (e.g., “1” for sand and “0 for clay in this study), the material properties will also be automatically assigned to new grids. The MODFLOW grids can also be easily updated when new well logs become available.

References

- Buono, A. 1983. The Southern Hills regional aquifer system of southeastern Louisiana and southwestern Mississippi, U.S. Geological Survey, Water-Resources Investigations Report: 83-4189.
- Dicken, Connie L., Nicholson, Suzanne W., Horton, John D., Foose, Michael P., and Mueller, Julia A.L. 2005. Integrated Geologic Map Databases for the United States: Alabama, Florida, Georgia, Mississippi, Louisiana, North Carolina, and South Carolina, U.S. Geological Survey, Open-File Report 2005-1323, Reston, VA.
- Elshall, A.S., F.T.-C. Tsai, and J.S. Hanor. 2013. Indicator Geostatistics for Reconstructing Baton Rouge Aquifer-Fault Hydrostratigraphy, Louisiana, USA. *Hydrogeology Journal*, 21, 1731-1747. doi:10.1007/s10040-013-1037-5
- Harbaugh, A.W. 2005. MODFLOW-2005, The U.S. Geological Survey Modular Ground-Water Model-the Ground-Water Flow Process. In Book 6. Modeling techniques, Section A. Ground Water, 253 p. Virginia: US Dept. of the Interior, US Geological Survey.
- McCulloh R.P., and P.V. Heinrich. 2012. Surface Faults of the South Louisiana Growth-Fault Province. In: Cox, RT, Tuttle M, Boyd O, Locat J (eds) *Recent Advances in North American Paleoseismology and Neotectonics east of the Rockies and Use of the Data in Risk Assessment and Policy*, Geological Society of America

- Tsai, F.T.-C., and W.W-G. Yeh. 2004. Characterization and Identification of Aquifer Heterogeneity with Generalized Parameterization and Bayesian Estimation, *Water Resources Research*, 40, W10102, doi:10.1029/2003WR002893.
- Tsai, F.T.-C. 2006. Enhancing Random Heterogeneity Representation by Mixing the Kriging Method with the Zonation Structure, *Water Resources Research*, 42, W08428, doi:10.1029/2005WR004111.
- US Congress. 1996. The safe drinking water act, Public Law, 104, 182.

Development of Total Maximum Daily Load for Dissolved Oxygen in Nutrient-Enriched Lowland Rivers

Basic Information

Title:	Development of Total Maximum Daily Load for Dissolved Oxygen in Nutrient-Enriched Lowland Rivers
Project Number:	2013LA92B
Start Date:	3/1/2013
End Date:	2/28/2014
Funding Source:	104B
Congressional District:	5th
Research Category:	Water Quality
Focus Category:	Models, Non Point Pollution, Water Quality
Descriptors:	
Principal Investigators:	Zhi-Qiang Deng

Publications

1. Zahraeifard, V., Deng, Z., and Malone, R. F. (2014). “Modelling Spatial Variations in Dissolved Oxygen in Fine-Grained Streams under Uncertainty.” Hydrological Processes, DOI: 10.1002/hyp.10144 (in press) (<http://onlinelibrary.wiley.com/doi/10.1002/hyp.10144/abstract>).
2. Zahraeifard, V. and Deng, Z. “Development of Total Maximum Daily Load for Dissolved Oxygen in Amite River.” World Environmental & Water Resources Congress, June 1 – 5, 2014, Portland, Oregon.

SYNOPSIS

Problem and Research Objectives

Nutrient-enriched lowland rivers in Louisiana are largely impaired due to low dissolved oxygen. In fact, the Louisiana's latest (2010) Integrated Report for water quality assessment indicates that about 45.7% of assessed rivers (155/339) are impaired due to low dissolved oxygen (DO) in terms of supporting fish and wildlife propagation (fishing). The US EPA requires states to develop Total Maximum Daily Load (TMDL) for pollutants causing impairments. While the DO load allocation requires the determination of sediment oxygen demand (SOD), the SOD in the organic-rich fluid mud (fluff) layer, commonly occurring in coastal Louisiana rivers, is rarely taken into account in TMDL development due to the lack of an effective modeling tool. The lack of an effective modeling tool for DO in nutrient-enriched lowland rivers causes high uncertainty in TMDL development and makes it challenging to restore impaired water bodies and thereby to comply with the Federal Clean Water Act. This is a critical regional and state water quality problem needing to be addressed.

The overall goal of this project is to develop an efficient and effective modeling tool for determining spatial and temporal variations in DO in nutrient-enriched lowland rivers and thereby to address the critical regional and state water quality problem. The proposed strategy is to test and demonstrate the new modeling tool for DO in the Lower Amite River and the Lower Tangipahoa River in southeast Louisiana. The Lower Tangipahoa River is on the latest US EPA and LDEQ 303(d) list for not supporting its designated use of fish and wildlife propagation due to low DO. Specific objectives of the project are: (1) to develop and test a new modeling tool, called VART DO-3L, for simulation of spatial and temporal variations in DO in nutrient-enriched lowland rivers. This objective will be addressed by the extension of the PI's VART model; and (2) to identify critical source areas of pollution in the Lower Tangipahoa River watershed, as shown in Figure 1.

Methodology

The objectives are accomplished by executing two tasks: (1) Development of triple-layer model for simulation of instream DO, and (2) construction of Google earth maps showing source locations of DO pollution. The proposed tasks are implemented by combining PI's proven VART model for solute transport in rivers, ArcGIS, Google Earth, and various data.

While this project focuses on the Lower Tangipahoa River and the Lower Amite River watersheds, the methods (particularly the VART DO-3L model) developed in this study can be easily extended to other watersheds in Louisiana and in other low relief regions. Therefore, this project has broader implications for environmental restoration and sustainability in Louisiana and in the nation as well.

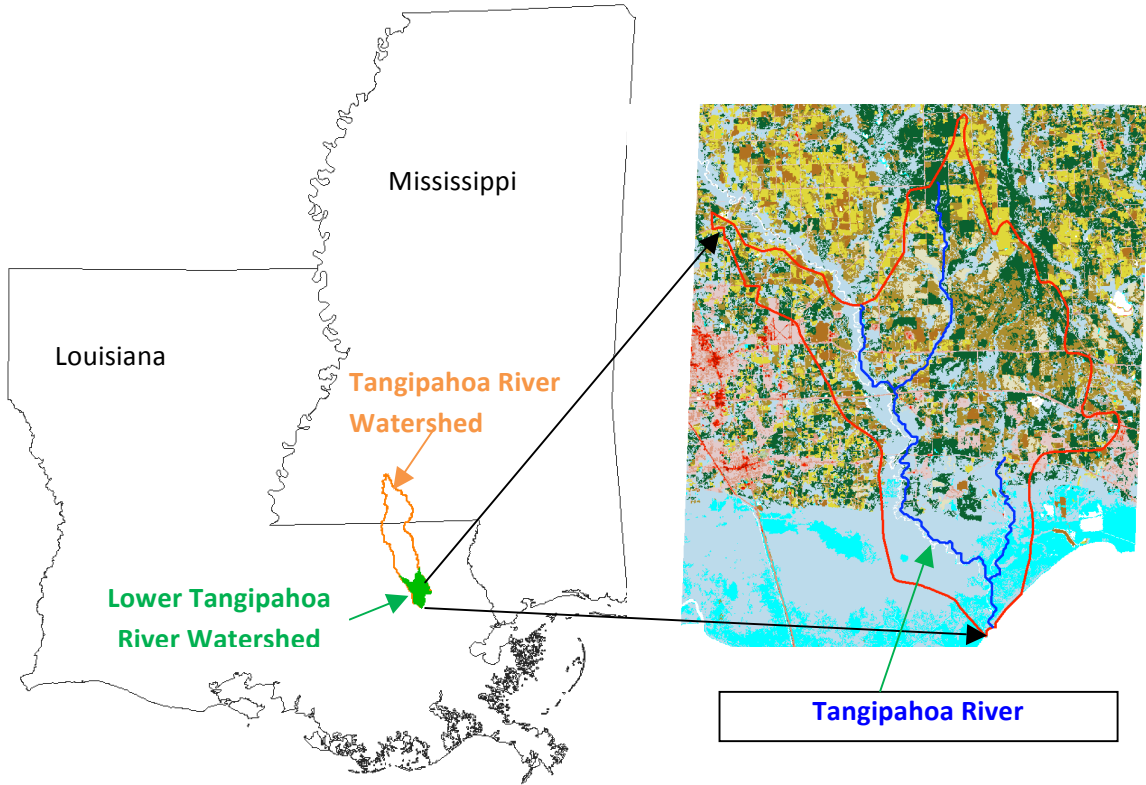


Figure 1. Map for the Tangipahoa River watershed.

PRINCIPAL FINDINGS AND SIGNIFICANCE

1. Mathematical Model for Spatial Variations in DO: VART DO-3L Model

(1) The triple-layer model is described mathematically with the following three equations:

$$\frac{\partial C}{\partial t} + U \frac{\partial C}{\partial x} = \frac{\partial}{\partial x} \left(E_x \frac{\partial C}{\partial x} \right) + \left(\frac{A_{adv} + A_{dif}}{A} \right) \left(\frac{I}{T_V} \right) (C_F - C) + K_2 (C_{sat} - C) - K_D L \quad (1)$$

$$\frac{\partial C_F}{\partial t} = \frac{I}{T_V} (C - C_F) - D_e \frac{\partial C_s}{\partial z} \Big|_{z=0} - \frac{P_{ws}}{\left(\frac{A_s}{A} \right) \cdot A} - R \quad (2)$$

$$\frac{\partial C_s}{\partial t} = D_e \frac{\partial^2 C_s}{\partial z^2} - \mu_o \quad (3)$$

where C , C_F , and C_s are DO concentration in water column, in the flocculent layer, and in consolidated stream bed [ML^{-3}], respectively; C_{sat} = saturation concentration of DO; U = average flow velocity [LT^{-1}] along x direction; E_x = longitudinal dispersion coefficient

$[L^2T^{-1}]$; t = traveling time [T]; x = distance in flow direction [L]; z = distance in vertical direction pointing downward [L]; K_D = biochemical oxidation rate of carbonaceous materials $[T^{-1}]$; L = BOD concentration $[ML^{-3}]$ in the water column; K_2 = reaeration coefficient $[T^{-1}]$; A = cross-sectional area of stream channel $[L^2]$; A_{adv} = advection-dominated storage zone (floculent layer) area $[L^2]$ with the thickness of δ_{adv} [L]; A_{dif} = diffusion-dominated storage zone (stream-bed sediment) area $[L^2]$ with the thickness of δ_{dif} [L]; $A_s = A_{adv} + A_{dif}$, T_V = residence time in storage zones (including A_{adv} and A_{dif}) [T]; D_e = effective diffusion coefficient in the bottom sediment layer; P_{ws} = wetted perimeter of stream channel; R = lumped reaction term representing SOD in the floculent layer; and μ_o = lumped reaction term denoting SOD in the bottom sediment. Eqs. (1) - (3) are utilized for simulation of spatial and temporal variations in DO in fine-grained streams, characterized by three layers, including water column, floculent layer, and consolidated stream bed. Equations (1) – (3) constitute the triple-layer (VART DO-3L) model. The VART DO-3L model provides an efficient and cost effective modeling tool for environmental and water resources management agencies to determine instream DO more accurately due to the incorporation of SOD in the fluff layer commonly occurring in nutrient-enriched lowland rivers and thus reduce the uncertainty in TMDL development and implementation.

- (2) The VART DO-3L model was first utilized to simulate vertical DO profiles in the Lower Amite River. Figure 2 shows normalized DO concentration profiles in the overlying water column, the floculent layer, and diffusive bottom sediment layer at Denham Springs station, Port Vincent station, and a third station in between that is 17 km downstream of Denham Springs station. The overall variation trends in the vertical DO profiles particularly in the bottom sediment layer are similar to those produced by using the concept of diffusive boundary layer above the sediment-water interface. The difference is due to the introduction of advection-dominated storage zone in this study with constant DO concentration throughout the floculent layer and water column layer.

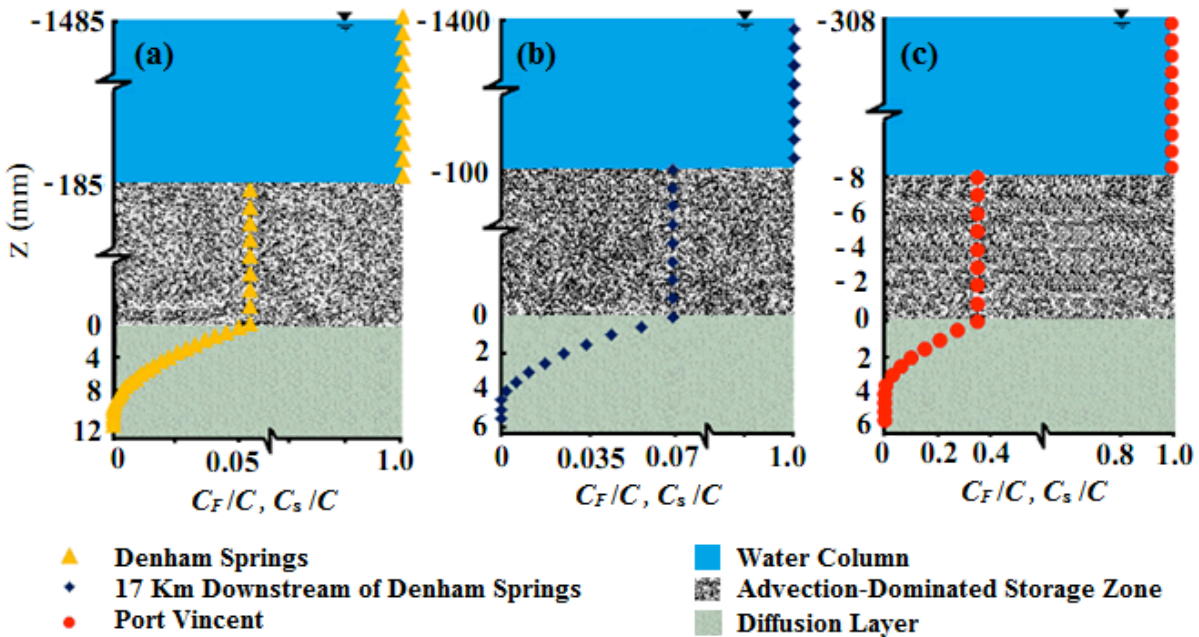


Figure 2. Vertical DO concentration ratio relative to DO concentration in water column at Denham Springs station (a), Port Vincent station (c), and a third station in between (b).

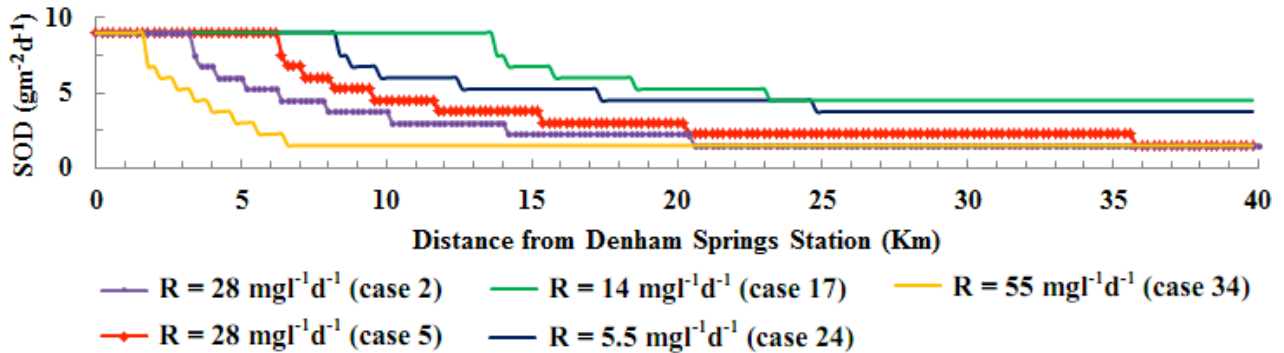


Figure 3. SOD variation along Amite River under different conditions.

- (3) The VART DO-3L model was utilized to simulate longitudinal SOD (Sediment Oxygen Demand) variations. Figure 3 shows simulated SOD variations along the Lower Amite River under five different cases. While a constant R value was adopted in the simulation for each case, the R value may actually vary along the river due to the change in the composition of sediment particle size and organic content in the sediment. Therefore, the actual variation in SOD along the river may be a combination of the cases. The upper reach close to the Denham Springs may have a relatively low R value like Case 24 while the lower reach close to the Port Vincent may have a high R value like Case 34. Anyway, it is the SOD that causes gradual reduction in DO from the upstream Denham Springs station (DO = 7.9 mg/l) to the downstream Port Vincent station (DO \approx 3 mg/l).
- (4) The VART DO-3L model was also used to simulate longitudinal DO variations. Figure 4 shows the DO reduction along the Amite River due to the SOD. The daily averaged DO data observed at Denham Springs and Port Vincent stations are also included. It can be seen from Figure 4 that the DO drops rapidly in the upper 10 km and then declines slowly in the lower portion of the river. The slow reduction in DO in the lower reach may be due to the low DO in water column and low DO concentration gradient across the sediment–water interface. Another mechanism possibly responsible for the slow reduction in DO is the increased reaeration at water surface, balancing the DO reduction due to SOD. Figure 4 indicates that the simulation errors vary in the range of +20% to –35% while the simulated DO level fits the observed one almost perfectly in panels (b) and (d).

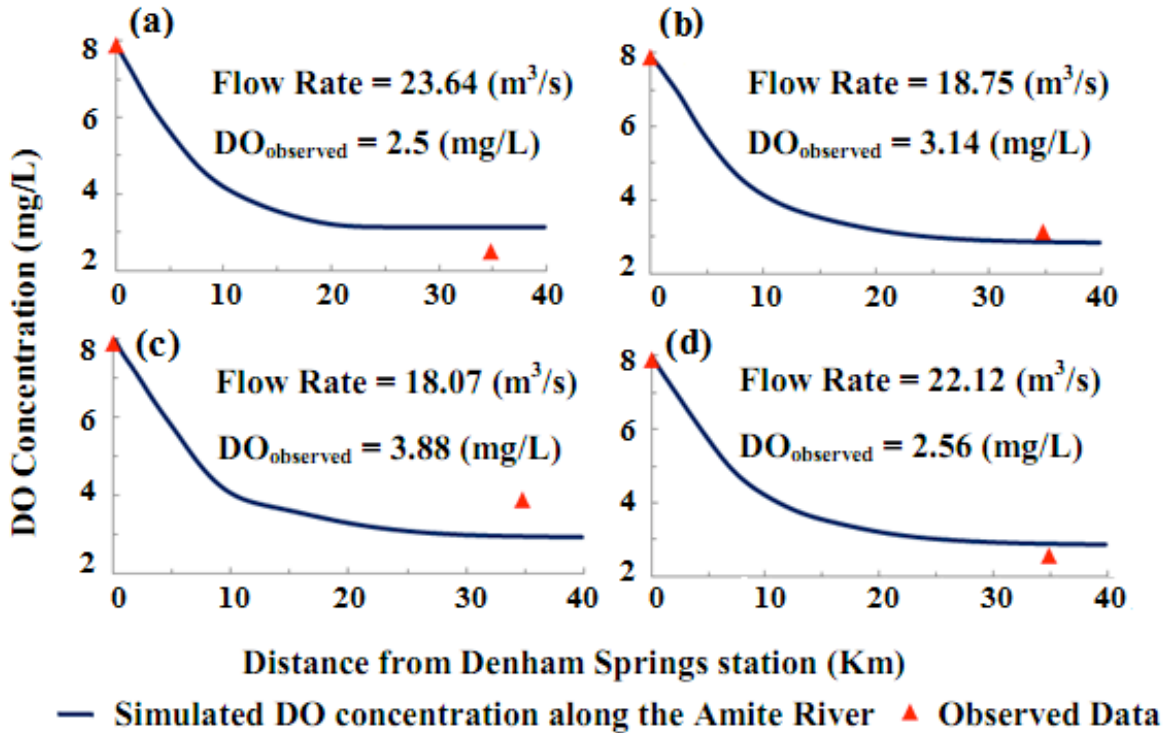


Figure 4. Longitudinal variations in DO along Amite River.

2. Identification of Critical Source Areas of Nonpoint Source Pollution in the Lower Tangipahoa River

(1) The variation in dissolved oxygen (DO) along the Tangipahoa River is mapped using ArcGIS and Google Earth to identify major source areas of DO-consuming contaminants, as shown in Figure 5. The map indicates that the DO level drops significantly downstream of the Chappepeela Creek confluence and particularly the Washley Creek confluence (not shown on the map, <http://itouchmap.com/?d=558193&s=LA&f=stream>), implying that the Chappepeela Creek watershed and particularly the Washley Creek watershed are potentially the major source areas of DO pollution to the Lower Tangipahoa River. The Chappepeela Creek and the Washley Creek collect runoff from dairy farms. The Runoff from dairy farms carries animal waste into the creeks, resulting in high bacteria counts and low dissolved oxygen concentrations.

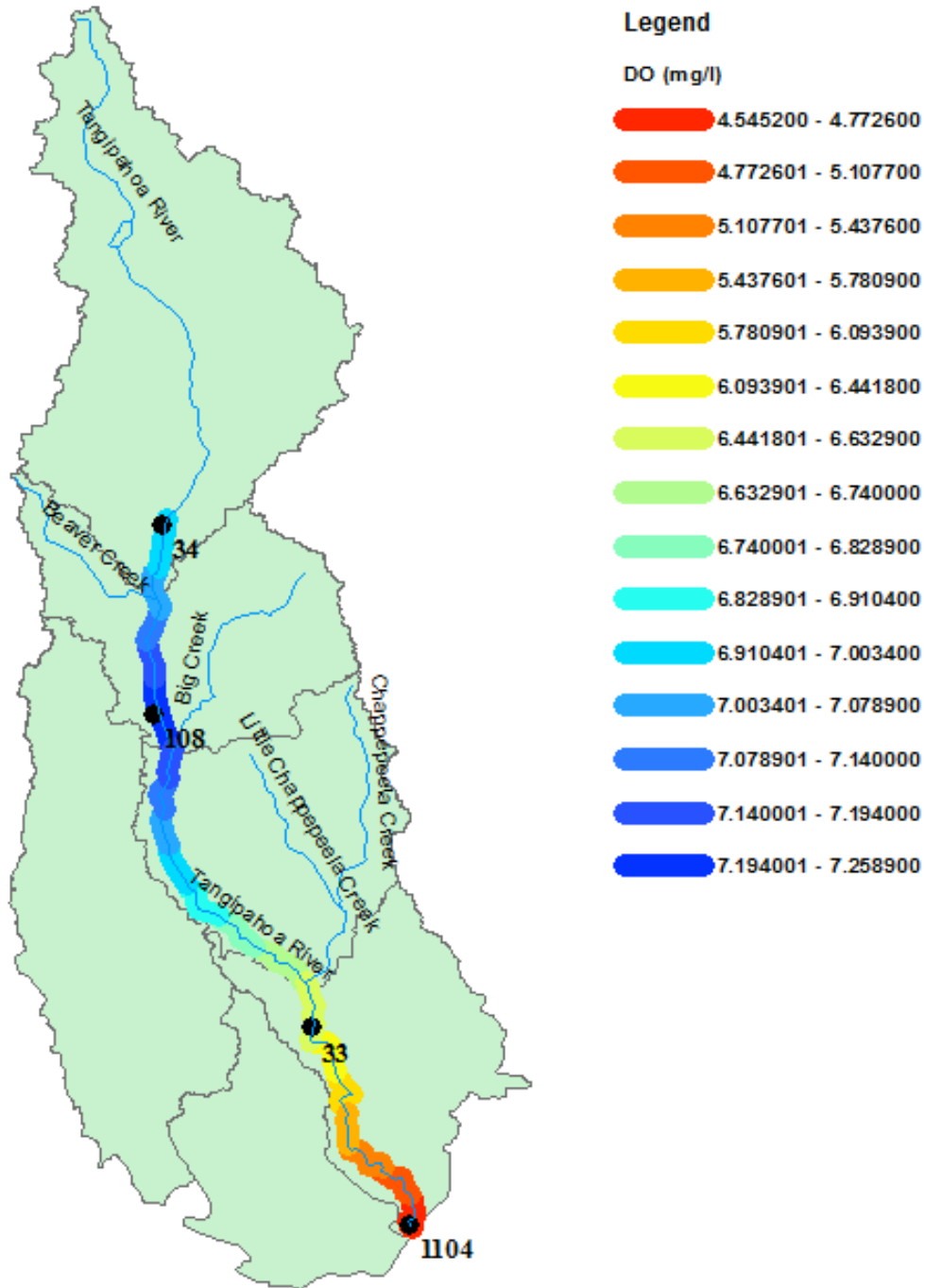
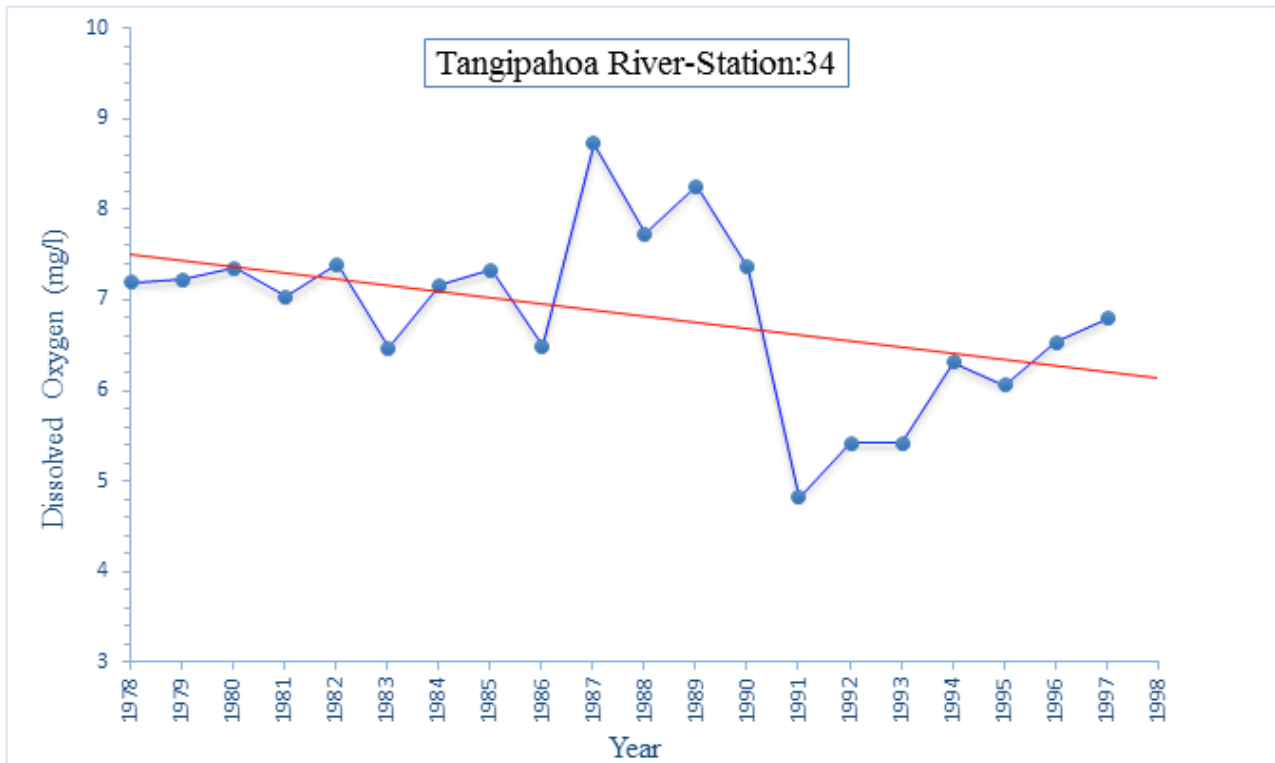
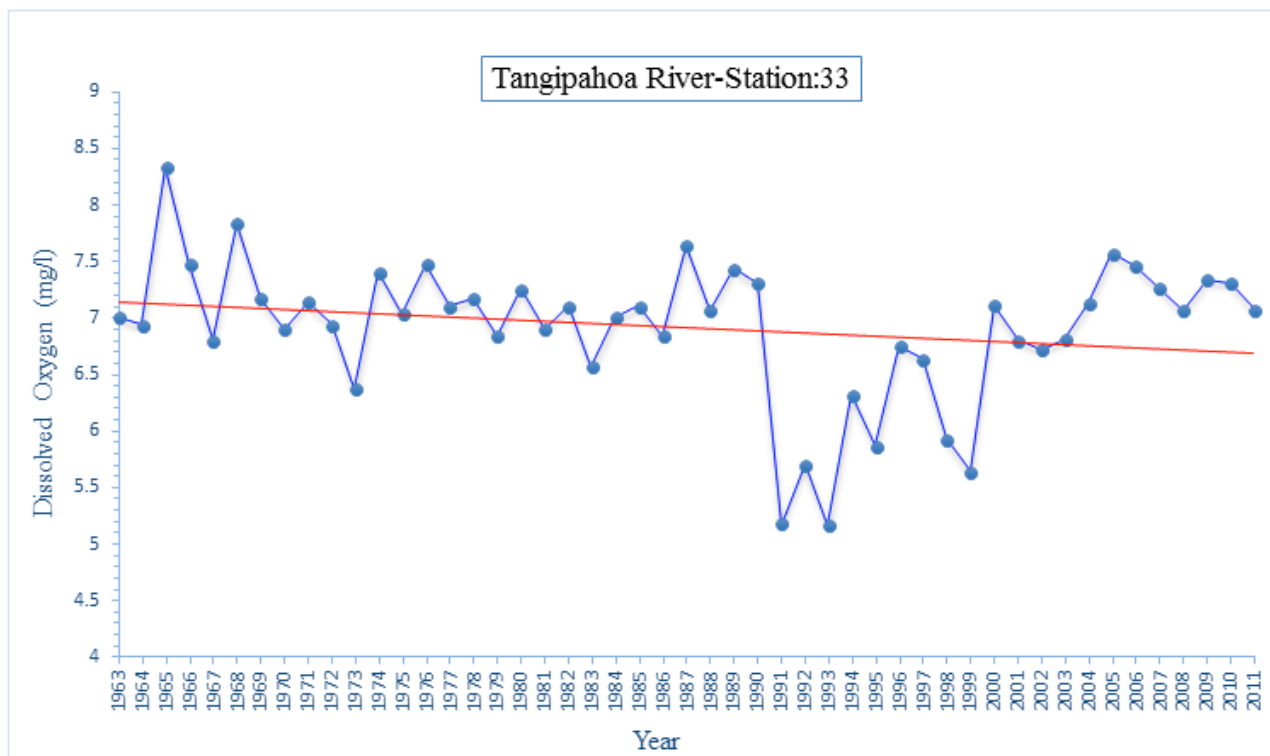
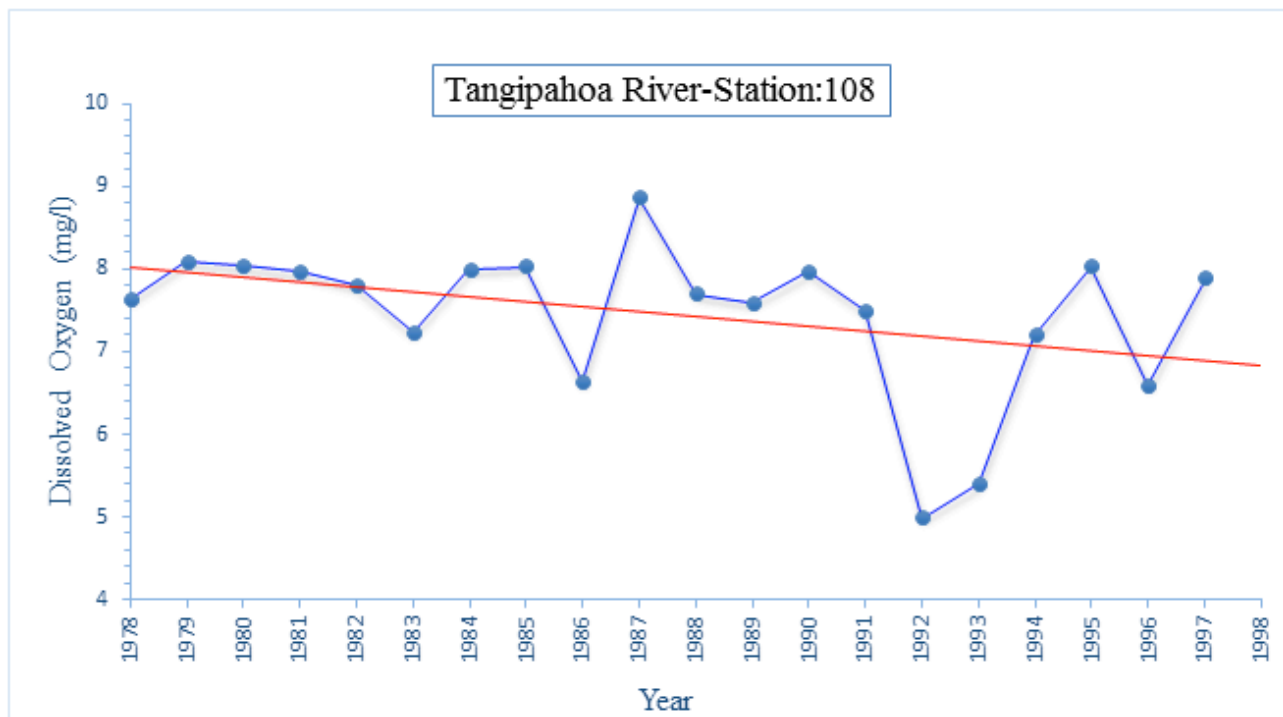


Figure 5. Map of Tangipahoa River watershed showing longitudinal DO variation along the Tangipahoa River and the critical source areas of DO-consuming contaminants in the Tangipahoa River subwatersheds.

(2) Figure 6 shows temporal variations in DO at four sampling stations, including 34, 108, 33, and 1104, along the Tangipahoa River. It can be seen from the four graphs that DO level exhibits a clear decreasing trend over the past decades at all the four stations. There was a significant drop in DO at the three upstream stations (including 34, 108, and 33) in

1991 - 1993. The implementation of Total Maximum Daily Load for DO has resulted in the improvement in the DO level at the three stations. However, the DO level at the downstream station 1104 remains lower than the minimum DO level of 5.0 mg/L required for maintaining aquatic life. The extremely low DO level at Station 1104 and in the lower portion of the river reach is attributed to the high BOD inputs from the Chappepeela Creek and the Washley Creek watersheds. The results are consistent with those from Figure 5. The last graph for Station 1104 in Figure 6 indicates again that the Chappepeela Creek and the Washley Creek watersheds are the major source areas of DO pollution to the Lower Tangipahoa River. TMDL implementation efforts for the Tangipahoa River should focus on the restoration of the Chappepeela Creek and the Washley Creek watersheds by implementing low impact development practices for dairy farms in the watersheds.





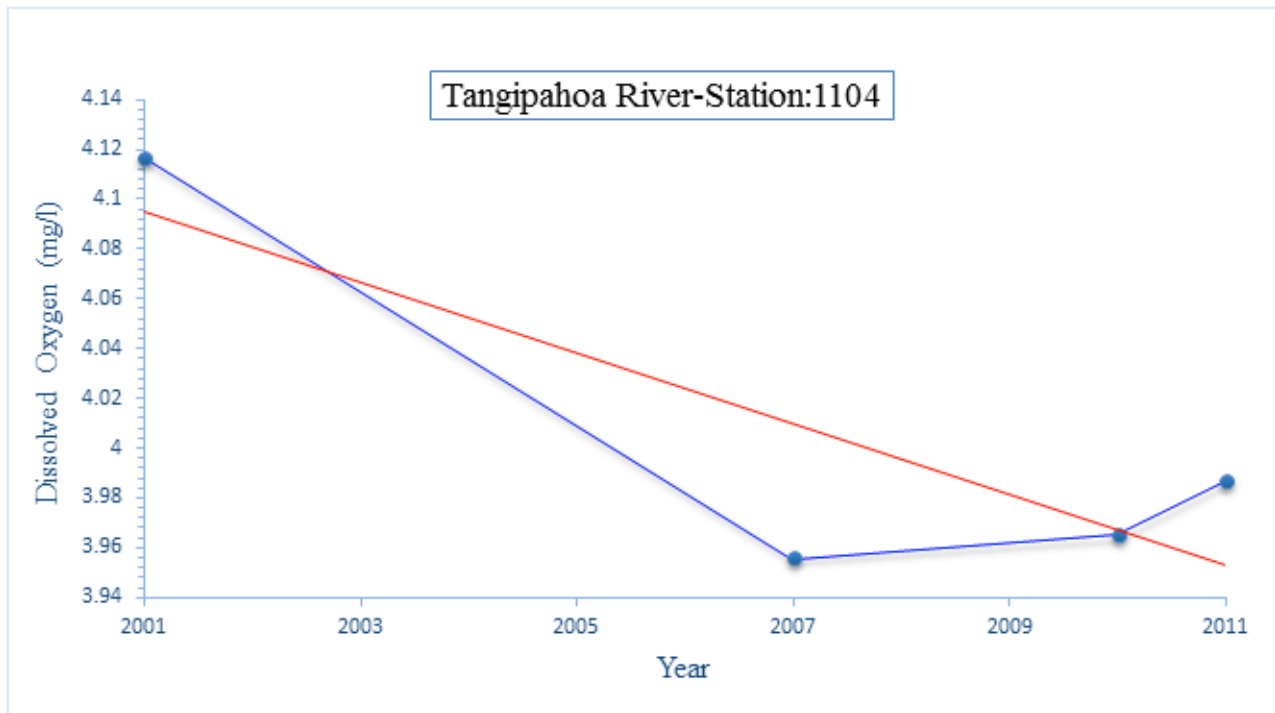


Figure 6. Temporal variations in DO at four monitoring stations, including 34, 108, 33, and 1104, along the Tangipahoa River.

INFORMATION TRANSFER

The findings and the VART DO-3L model developed in this project for simulation of spatial-temporal DO variations and identification of contaminant source areas will be transferred to the Louisiana Department of Environmental Quality for pollutant TMDL development and implementation and thereby for the restoration of the nutrient-enriched lowland rivers.

Sustainable Iron Removal from Groundwater Supporting Aquaculture

Basic Information

Title:	Sustainable Iron Removal from Groundwater Supporting Aquaculture
Project Number:	2013LA93B
Start Date:	3/1/2013
End Date:	2/28/2014
Funding Source:	104B
Congressional District:	5th
Research Category:	Engineering
Focus Category:	Agriculture, Groundwater, Treatment
Descriptors:	
Principal Investigators:	Ron Malone, Donald Dean Adrian

Publications

There are no publications.

Synopsis

Problem and Research Objectives

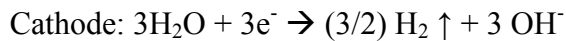
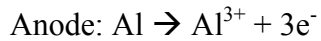
This project built scientific foundation to facilitate the development of simplified approaches to the removal of iron in a rural environment. The targeted beneficiary of this effort is the aquacultural industry in the state. Aquacultural facilities in the state generate over 100 million dollars of product including industries such as catfish, tilapia, turtles, alligators, soft crabs, and crayfish. Many of these facilities are located in rural areas and their processes require a relatively high volume of freshwater from wells. As well water is considered disease free; it is the preferred water source. However, iron is toxic to most fish and crustaceans at low levels and is seen as problematic in a number of locales. Iron contamination of wells, for example, has been cited as a factor inhibiting soft crayfish production as early as 1990 (Culley & Doubinis-Grey, 1990). It is estimated that 8 percent of the Louisiana groundwater withdrawals are used for aquacultural purposes (Todd et al., 2008). With usage estimated at nearly 150,000 acre-feet/year, Louisiana is ranked fifth in the country for aquaculture groundwater withdrawals (Hutson et al., 2004). However, iron contamination is a problem in many parts of the state, as aquatic animals, fish and crustaceans, are sensitive to free iron concentrations in water, with concentrations above 0.15 ppm generally considered toxic (Timmons & Ebeling, 2010). Iron is a common contaminate in Louisiana groundwaters where it is rapidly released from iron rich soils wherever oxygen depletion leads to ferric iron reduction. LADEQ (2006) reports several of our major aquifers display mean iron concentrations above 1 ppm . The two main alluvial aquifers display mean values over 5 ppm (Red River) and 8 ppm (Mississippi River). Iron is also a common problem in shallow rural wells which are impacted by organically rich surface soils. Although iron removal techniques are well identified (Tchobanoglous et al., 2003), the aquacultural industry generally lacks a cost effective means of treating the high volumes of water their industry demands. Similar iron problems exist in adjacent states (Todd et al., 2008).

Floating bead filters that integrate biofiltration and physical filtration into a single unit are known as “bioclarifiers”. These units have been used successfully to simplify water treatment in recirculating aquaculture systems. In recent years, traditional treatment sequences have been reduced from several components to as little as two (a bioclarifier and an airlift), which operate with dramatically less impact on the environment. Energy consumption has been reduced by over fifty percent compared to recirculating designs of the late 1990’s. These units are washed pneumatically, refiltering their own backwash waters, reducing the discharged waste water to less than 1 percent of a similarly sized sand filter (Malone and Gudipati, 2006).

Adoption of the floating bead technology will be dependent on the impact of the oxidation step on the particle size distribution of the iron hydroxides produced. Floating bead filters using standard 2-3 mm spherical bead can achieve 100 percent removal of particles above 50 microns (Drennan et al., 1994). Removal efficiencies decline to about 30 percent per pass when the particle size drops to the 5-10 micron range. The bead filters removal break point (50 microns) is almost midway between a sand filter (about 20 microns) and a settling tank (100 microns) (Ahmed 1996).

Application of an electro-coagulation technique was anticipated to accelerate the rate of formation, and ultimately, the size of floc produced in an iron removal process. Electrocoagulation of iron has been proved as an effective method of iron removal (Ghosh et al., 2008). The hydroxide flocs formed in the process act as adsorption sites for iron. EC process has gained importance because of its high removal efficiency, no use of chemicals, no secondary harmful disposal pollutant generation, and less time requirement. In the process of electrocoagulation, sacrificial metal anode dissolves thus, generating the coagulant species.

Immediate generation of hydrogen can be seen at cathode. This sacrificial anode is responsible in the precipitate formation and adsorption of contaminants from water. Reactions at respective electrodes are shown here (Aluminum electrode has been used) (Ghosh et al., 2008):



The amount of Aluminum (Al^{3+}) released at different currents is calculated according to Faraday's second law of electrolysis:

$$x \text{ (gm)} = \frac{A \times T \times MW}{96484.56 \times e^{-}}$$

Where;

x : mass of substance released or consumed in grams

A : Amount of current passed in Amperes

T : Time for which the current was passed in seconds

MW : Molecular weight of the substance released or consumed

e^{-} : number of valance electrons in 1 mole of substance

This project evaluated the application of an electro-coagulation and floating bead filter combination to the iron removal for aquaculture. Specific objectives addressed included:

- 1) Determine the likely cause, and a means of avoidance, of mineral coatings that caused the loss of buoyancy in early floating bead filter iron removal applications.
- 2) Define operational guidelines for key parameters (aluminum dosage, flow, recirculating flow, pH, and retention time) required to reduce total iron levels to a level (1 ppm) safe for aquacultural applications.

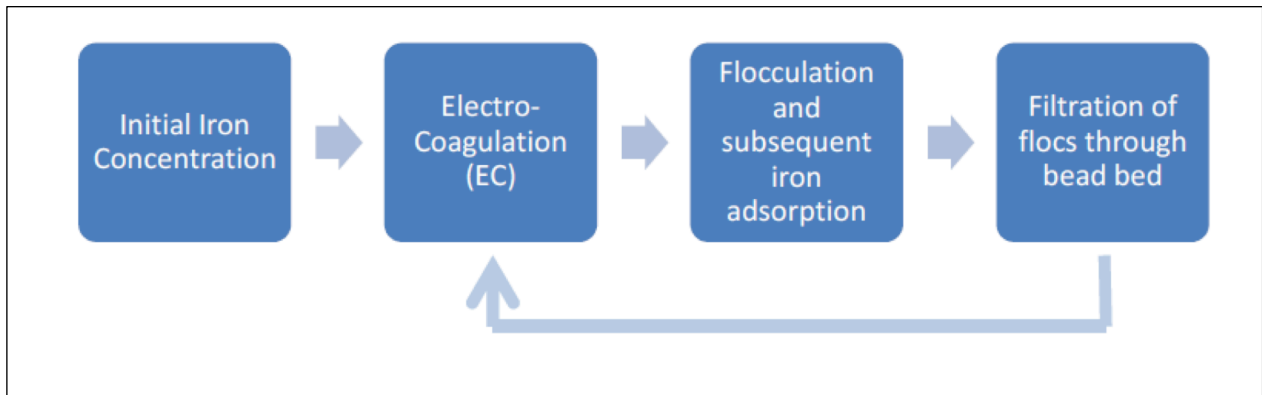
Methodology

Iron removal from groundwater has caused problems while using floating bead filters. Failure of one such filter installed on New Roads on Mississippi River due to heavy iron coating around the polyethylene beads lead to further investigation of the issue. Literature review suggested that the coat formation around media is caused by adsorption mechanism which is the adsorption of contaminant particles to the media surface (Benjamin, 2013; Sharma, 2001). Dissolved oxygen content and pH are the key factors governing the coat formation. Ferrous iron gets adsorbed onto the beads which are then oxidized to ferric in the presence of oxygen.

To check on the iron coat formation on the beads a small batch experiment was conducted. The experiment was carried out in a 1.5 Liter volume capped plastic container. The container was first filled with 1 liter deionized water. The dissolved oxygen and pH of the water was then recorded. Sodium sulfite was then added to this water to scavenge out the dissolved oxygen. After dropping the dissolved oxygen content, the pH was monitored. The pH of water shoots up to about 8 after adding sodium sulfite to it. The pH was then lowered and set to 6.5 by bubbling in CO₂ gas. Thus, the initial conditions for starting the experiment are a pH of 6.5±0.1 and dissolved oxygen amount between 0 to 0.1. Iron in the form of ferrous sulfate and ferrous chloride were tested individually. Five grams of these which is equivalent to 1.84 gm-Fe/L and 2.2 gm-Fe/L of these were added to the container and mixed thoroughly. Dry polyethylene floating beads weighing 200 grams were then added to the container. Total bead surface area available for adsorption was 10054 cm². The beads were kept moving on a magnetic stirrer (Corning PC-220 Hot Plate/Stirrer) set at the lowest speed permitted by the machine which is 60 rpm. Experiment was run for three days. At the end of three days, air was bubbled in the container for 10 minutes to increase the oxygen content of water. Beads were then separated out

and kept for drying. The dried beads were then weighed with increases in weight attributed to ferric hydroxide accumulations.

The apparatus used for running the iron removal experiments consisted of a 4 foot long, 6 inch diameter (ID) acrylic coagulation tank and a 3 foot long, 4.5 inch (ID) acrylic pipe with a 9 inch bead bed. The two cylinders were connected by $\frac{3}{4}$ inch PVC piping. Water from the electrocoagulation tank was fed by gravity through the bead bed, then was lifted back to the electro-coagulation tank by a centrifugal pump. The effective system volume was 26.1 liters. The pH of water was generally maintained between 8.0 ± 0.3 by adding sodium bicarbonate. Temperature was set to 25°C . Iron was added in the form of $5 \text{ mg-Fe}^{3+}/\text{L}$ of ferric as ferric chloride. Flat aluminum electrodes having dimension $1\text{-}1/2'' \times 1/16'' \times 46''$ were used in the electro-coagulation. These plates were connected to a Mastech DC power supply. The experiments were run in a recirculating batch mode with an initial iron concentration of 5 mg-



Fe^{3+}/L . Flow chart for the batch mode with recirculating flow is given in Figure 1.

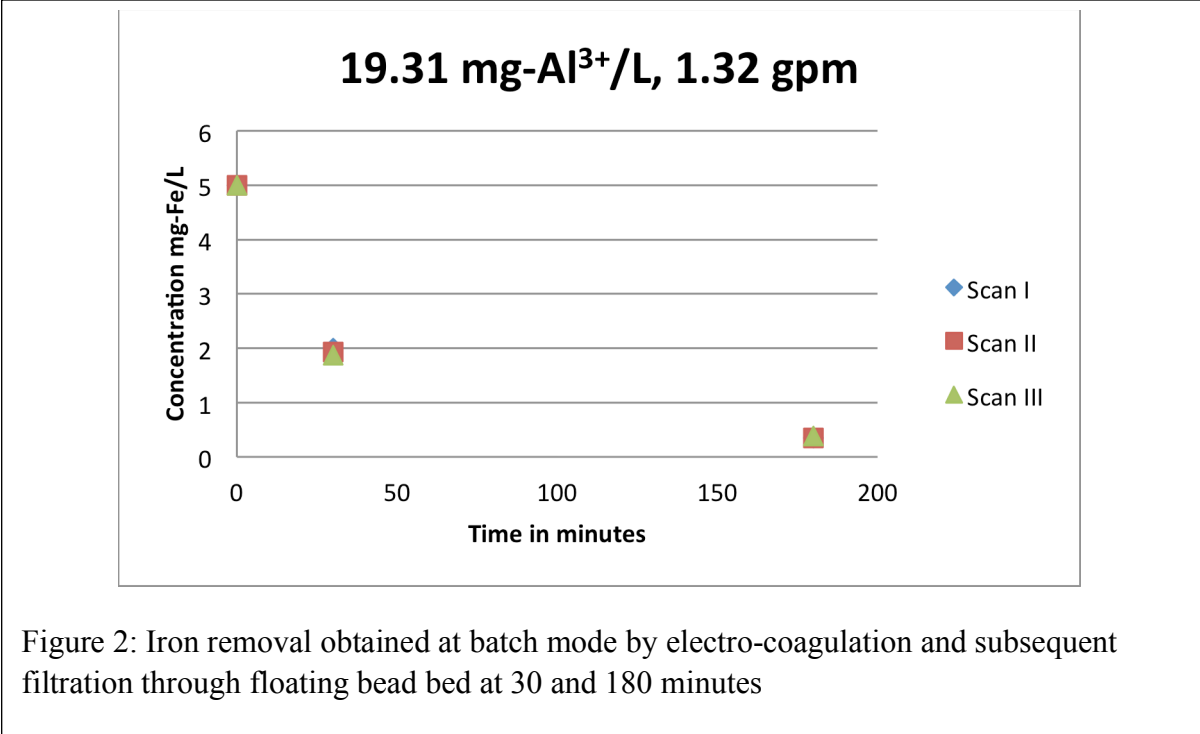
Figure 1: Flow chart representing experimental steps under batch mode of influent with an internally recirculating flow

Results and Discussion

The results of the iron coating studied confirmed that conditions commonly associated with shallow Louisiana groundwaters, i.e. a $\text{pH} < 7.0$ and low dissolved oxygen, are conducive to

coating of plastic beads. Visible iron coatings were observed when the beads were exposed to iron rich waters while the pH was near 6.5. Mineral accumulation rates ranged from $0.033\text{mg}/\text{cm}^2$ and $0.0431\text{mg}/\text{cm}^2$ after three days dosed with ferrous sulfate and ferrous chloride, respectively. Accumulations were not observed, however, whenever the pH was maintained above or whenever the water was well aerated. These findings are consistent with a two-step coating process. First ferrous iron precipitates on the surface as ferrous hydroxide, then as oxygen becomes available the surface hardens as the ferrous hydroxides are converted to ferric hydroxides. Polyethylene beads do not have any negative surface charge and do not attract the positive ferrous ions as compared to sand which readily adsorbs iron to its surface because of its negative surface charge. While arguably pre-coating plastic beads could improve iron removal rates, it is clear that the sinking of beads by iron coating can be avoided by well aerating waters prior to filtration. This approach strips the elevated carbon dioxide commonly associated with shallow groundwaters raising the pH while promoting the rapid formation of ferric iron hydroxides.

Success of the iron removal strategy evaluated here is predicated on the electrocoagulation in a unit's ability to form floc particles in a size range (>30 microns) that is readily removed by a bed of 2-3 mm beads (Ahmed, 1996). To further compensate for weak lower end removal capabilities the water is recirculated through the process providing for multiple filtration passes. As Figure 2 illustrates, the use of electro-coagulation with a recirculating floating bead filter is capable of reproducibly removing iron down to about $0.3\text{ mg}/\text{L}$. However, the process requires a treatment process of about 180 minutes. Figure 2 represents the results obtained on passing 3 amperes of current for 30 minutes. The flow rate was set to 1.32 gpm ($12\text{ gpm}/\text{ft}^2$ of filtration flux rate).



This process proved to be relatively insensitive to dosage as seen in Figure 3 with the best removal being observed at lower Al³⁺ dosage rates tested (6.43 mg-Al³⁺/L). These results are consistent with the Metcalf and Eddy Inc., 1991 definition of 1.8 to 5.4 mg-Al³⁺/L as the optimum range for floc formation in water treatment plants using alum. Since the floc was constantly being removed as the electro-coagulating plates provided the dose over a 30 minute period, the peak aluminum dosage undoubtedly fell within the optimum range. Increasing the aluminum dosage by raising the amperage dramatically improved aluminum hydroxide floc production, but, had little impact on iron removal rates.

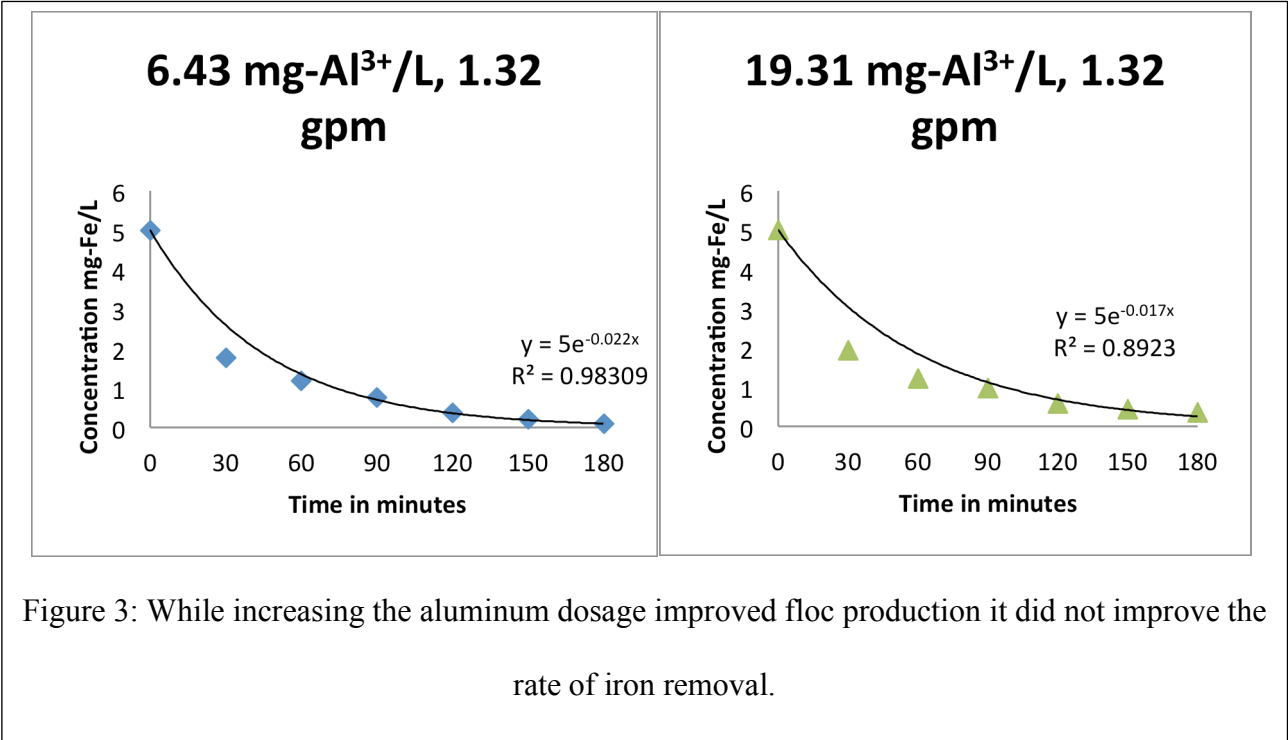


Table 2 presents the results of several comparable iron removal runs conducted at background pH of about 8.2 dosed initially with 5 mg-Fe⁺⁺⁺/L. Iron removal below the 1 ppm target was not achieved within 30 minutes under any conditions. As illustrated here, it was achievable with a retention time of 180 minutes. After 30 minutes the water in the system was passed through a 0.2µm pore size filtration process revealing that the residual iron is particulate in form. Yet, variation in the recirculating flow, which presumably would improve the floating bead bed's ability to small particles by increasing the number of filtration passes, was found to have little impact on the process efficiency. These observations indicate that the aluminum electrocoagulation process is limited in its ability to scavenge small iron precipitates, or, that the process is time limited.

Table 2: Average of iron removals obtained at different system conditions with initial iron concentration as 5 mg-Fe³⁺/L, temperature 25°C and 30 minutes of current flow.

Current (Amps)	Equivalent Al ³⁺	pH	Recir. Flow	Internal turnover	Residual Iron* (mg-Fe ³⁺ /L)
----------------	-----------------------------	----	-------------	-------------------	---

	dosage mg-Al ³⁺ /L		(gpm)	time (min)	30 min	180 min	Filtered **
1	6.43	8.25	0.11	43	1.83	--	0.11
1	6.43	8.27	0.33	14.3	2.11	--	0.06
1	6.43	8.31	1.32	3.59	1.66	0.10	0.11
3	19.31	8.28	0.11	43	1.77	--	0.12
3	19.31	8.16	0.33	14.3	2.10	--	0.29
3	19.31	8.22	1.32	3.59	1.61	0.36	0.31
6	38.62	8.20	0.11	43	1.81	--	0.07
6	38.62	8.22	0.33	14.3	2.25	--	0.21
6	38.62	8.26	1.32	3.59	2.04	--	0.19
* means of triplicates ** Filtered iron concentration (through 0.2µm pore size) at the end of 30 minutes							

In summary, the results of this work provide guidance for the avoidance of the formation of iron precipitates on the surface of floating beads. The results suggest that thoroughly aerating well water before contact with the bead bed will avoid the problem of coating, then sinking floating plastic beads. The combination of electro-coagulation with aluminum plates in recirculation with a floating bead bed was shown to be capable of removing residual iron concentrations to a level well below a 1 ppm iron level considered suitable for aquaculture applications. However, without pH adjustment, the process treatment time was long with approximately 75 minutes being required to reach 1 ppm for the best combination of operational parameters. A wide range of operational conditions were capable of achieving the 1 ppm objective in about 120 minutes. This extended treatment time would limit practical application

to low flow demand requirements associated with recirculating aquaculture systems. The size of reactor tanks limiting its value for high demand applications (ponds or flow through tank systems). The extended treatment time is attributed to the formation of extremely small iron precipitates that showed little affinity for aluminum flocs formed by the electro-coagulation process. These fine precipitates were only slowly removed by 1-2 mm bead beds employed.

References

- Ahmed, Helal. *The Effects of Fluxrate and Solids Accumulation on Small Size Particle Accumulation in Expandable Granular Bead Filters*. Masters Thesis, Louisiana State University, 1996. Baton Rouge
- Benjamin Mark M. and Lawler Desmond F., *Water Quality Engineering: Physical/ Chemical Treatment Processes*, John Wiley & Sons, Inc., 2013
- Culley D. and Doubinis-Gray L. *A Production Manual Culture of the Louisiana Soft Crawfish*. Louisiana Sea Grant College Program Center for Wetland Resources Louisiana State University. Baton Rouge, LA. 1990
- Hutson, S. Barber, N. Kenny, J. Linsey, K. Lumia, D. Maupin, M. *Estimated Use of Water in the United States 2000*. United States Geologic Survey. March, 2004.
- Malone, R.F. and Gudipati. S. Airlift-PolyGeysers Combination Facilitates Decentralized Water Treatment in Recirculating Marine Hatchery Systems. In Proceedings of the 34th US Japan Natural Resources Panel Aquaculture Symposium, San Diego, California. 2006.
- Sharma Saroj Kumar, *Adsorptive Iron Removal from Groundwater*, Dissertation, Wageningen University, Delft, Netherlands, December 2001.
- Tchbanaglou G. Burton F. and Stensel H. *Wastewater Engineering Treatment and Reuse*. New York: McGraw Hill. 2003.
- Timmons, M. Ebeling, J. *Recirculating Aquaculture*, Second Edition. Ithica, NY: Cayuga Aqua Ventures. 2010.
- Todd et al. *State of the Ground Water Report*. Ground Water Center U.S. Environmental Protection Agency Region 6. January, 2008.

Information Transfer Program Introduction

None.

USGS Summer Intern Program

None.

Student Support					
Category	Section 104 Base Grant	Section 104 NCGP Award	NIWR-USGS Internship	Supplemental Awards	Total
Undergraduate	3	0	0	0	3
Masters	2	1	0	0	3
Ph.D.	2	5	0	0	7
Post-Doc.	1	0	0	0	1
Total	8	6	0	0	14

Notable Awards and Achievements

LWRRI advised response agencies and conducted research on the spill • Advised the state through the Horizon Science and Engineering Review Team (H-SERT), a group of academic experts who worked with state trustees on the response. LWRRI Director Pardue led one of the standing committees in H-SERT and participated by reviewing and commenting on dozens of documents and plans. LWRRI set up a collaborative web review process for H-SERT which allowed participating by academics across the state. Pardue also participated in helicopter tours with the lead trustee agency, the Office of Coastal Protection and Restoration. • Dr. Pardue has also provided comments on many plans and remediation strategies ongoing through 2014 • Service on national American Petroleum Institute committee on “Use of Dispersants in the Deep Ocean” • LWRRI Director Pardue is coordinating research and damage assessment for the Wisner Donation property in Lafourche Parish, one of the 10 largest landowners in the state. The Wisner Donation property includes 35,000 acres including Fourchon Beach. Dr. Pardue has travelled to Wisner areas to conduct research an average of once per week since October 2010. • Received research funding from LSU GOMRI BP fund and Wisner Donation • 23 students (undergraduate, MS and PhD) have been involved in this activity to date.

LWRRI research successfully predicts norovirus outbreak Dr. Zhiqiang Deng, associate professor of Water Resources and Coastal Engineering in the Department of Civil & Environmental Engineering, is using satellite data from the National Aeronautics and Space Administration (NASA) to develop better tools for predicting and preventing seafood contamination. In 2013, Deng and his research group became the first group of scientists in the world to predict oyster norovirus outbreaks in advance when they correctly predicted the outbreak in Cameron Parish Oyster Harvesting Area 30 weeks before it occurred. Deng’s research, conducted in collaboration with the Louisiana Department of Health and Hospitals (LDHH), is a major breakthrough in protecting public health.